

Higgs Boson Exempt No-Scale Supersymmetry and its Collider and Cosmology Implications

Jason L. Evans, David E. Morrissey, James D. Wells

*Michigan Center for Theoretical Physics (MCTP)
Physics Department, University of Michigan, Ann Arbor, MI 48109*

August 15, 2018

Abstract

One of the most straightforward ways to address the flavor problem of low-energy supersymmetry is to arrange for the scalar soft terms to vanish simultaneously at a scale M_c much larger than the electroweak scale. This occurs naturally in a number of scenarios, such as no-scale models, gaugino mediation, and several models with strong conformal dynamics. Unfortunately, the most basic version of this approach that incorporates gaugino mass unification and zero scalar masses at the grand unification scale is not compatible with collider and dark matter constraints. However, experimental constraints can be satisfied if we exempt the Higgs bosons from flowing to zero mass value at the high scale. We survey the theoretical constructions that allow this, and investigate the collider and dark matter consequences. A generic feature is that the sleptons are relatively light. Because of this, these models frequently give a significant contribution to the anomalous magnetic moment of the muon, and neutralino-slepton coannihilation can play an important role in obtaining an acceptable dark matter relic density. Furthermore, the light sleptons give rise to a large multiplicity of lepton events at colliders, including a potentially suggestive clean trilepton signal at the Tevatron, and a substantial four lepton signature at the LHC.

Contents

1	Introduction	2
2	Generating Small Scalar Soft Terms	5
2.1	Models	5
2.2	The Scale of M_c	7
3	Mass Spectrum and Constraints	9
3.1	One-Loop Analysis	9
3.2	Parameter Space Scans	10
3.3	Constraints from $(g - 2)_\mu$	13
3.4	Constraints from the Higgs Boson Mass	14
4	Dark Matter and Cosmological Signals	15
4.1	Neutralino LSP Relic Density	15
4.2	Direct and Indirect Detection of Dark Matter	18
5	Collider Signatures	21
5.1	Trilepton Signature at the Tevatron	22
5.2	Signals at the LHC	24
6	Discussion	28

1 Introduction

Supersymmetry is a well-motivated way to extend the standard model (SM). Most impressively, supersymmetry can stabilize the large disparity between the size of the electroweak scale and the Planck scale [1]. In addition, the minimal supersymmetric extension of the SM [2], the MSSM, leads to an excellent unification of the $SU(3)_c$, $SU(2)_L$, and $U(1)_Y$ gauge couplings [3] near $M_{GUT} = 2 \times 10^{16}$ GeV, a scale that is large enough that grand-unified theory (GUT) induced nucleon decay is not a fatal problem. The MSSM also contains a new stable particle if R -parity is an exact symmetry. This new stable particle can potentially make up the dark matter.

The main obstacles facing supersymmetric extensions of the SM come from the requirement that supersymmetry be (softly) broken. To preserve the natural supersymmetric

hierarchy between M_W and M_{Pl} , every MSSM operator that breaks supersymmetry should be accompanied by a dimensionful coupling of size less than about a TeV. However, for a generic set of soft terms of this size, consistent with all the symmetries of the theory, the amount of flavor mixing and CP violation predicted by the model is much greater than has been observed. Instead, the experimental constraints require that the soft terms be nearly flavor-diagonal in the super-CKM basis [4], and that nearly all the independent CP violating phases be very small [4, 5], or finely-tuned to cancel [6]. From the low-energy perspective, it is not clear why this should be so.

A number of approaches to the supersymmetric flavor and CP problems have been put forward, such as adding new flavor symmetries to the MSSM [7], or mediating supersymmetry breaking through gauge interactions [8] or the superconformal anomaly [9]. These models also face new difficulties. New flavor symmetries typically require additional matter fields and hence the complications that go with them. Gauge mediation generates flavor-universal soft masses and trivially small A terms, but does not fully solve the CP problem, and makes it difficult to generate both the μ and $B\mu$ terms with the correct size. Anomaly mediation in its most simple form suffers from tachyonic slepton soft masses [9]. A more radical approach to the flavor and CP problems is to push the scale of the soft supersymmetry breaking scalar couplings to be much larger than the electroweak scale [10, 11]. If this is done while keeping the gauginos relatively light, it is possible to preserve gauge unification and a good dark matter candidate [12]. Of course, supersymmetry would no longer directly solve the gauge hierarchy problem if the scalar superpartners are very heavy.

Another way to address the supersymmetric flavor problem, and the one we consider in the present work, is to have the soft scalar masses and the A terms vanish simultaneously at a scale M_c [13]. If this scale is much larger than the electroweak scale, and if the gaugino masses do not vanish at M_c , non-zero values for the scalar soft terms will be generated by radiative effects as the theory is evolved to lower energies. Since the scalar soft terms thus induced are family-universal, the resulting soft spectrum does not have a flavor problem. The supersymmetric CP problem is also improved but not solved by this approach. Besides the CKM phases, the only remaining phases are those of the gaugino soft masses, and the μ and $B\mu$ terms. If the gaugino soft mass phases are universal, there are three new phases of which two can be removed by making field redefinitions [5]. The remaining phase can be eliminated as well within particular models [14].

Near-vanishing soft scalar terms can arise in a number of ways. The canonical examples are the no-scale models of gravity mediated supersymmetry breaking. In these models, the absence of scalar soft terms is related to the flatness of the hidden sector potential that allows the gravitino mass to be determined by loop-corrections due to light fields [15]. A more recent construction that leads to near-vanishing soft scalar operators is gaugino-mediated supersymmetry breaking [14]. Here, the MSSM chiral multiplets are separated from the source of supersymmetry breaking by an extra-dimensional bulk, while the gauge multiplets propagate in the bulk. Locality in the extra dimension(s) leads to gaugino masses that are much larger than the scalar soft terms. Small scalar soft terms can also be obtained from strong conformal dynamics in either the visible or the hidden sectors. In these constructions, the conformal running suppresses the scalar soft terms exponentially relative to the gaugino

soft masses [16].

The main difficulty with very small input scalar soft masses is that the lightest SM superpartner particle is usually a mostly right-handed slepton, which can be problematic for cosmology. This is nearly always the case if gaugino universality is assumed to hold above M_{GUT} , and $M_c \leq M_{GUT}$. On the other hand, if M_c is an order of magnitude or more above M_{GUT} (with gaugino universality), the lightest superpartner becomes a mostly Bino neutralino. A viable low-energy spectrum can be obtained in this way [17, 18]. For $M_c \leq M_{GUT}$, a neutralino LSP can be obtained by relaxing the requirement that all soft scalar terms vanish at M_c . One such generalization that does not re-introduce a flavor problem is to allow the Higgs soft masses $m_{H_u}^2$ and $m_{H_d}^2$ to be non-zero at M_c . These soft masses contribute to the running of the slepton masses through a hypercharge Fayet-Iliopoulos D -term, and can push the slepton masses above that of the lightest neutralino [18, 19, 20].

In the present work, we study the phenomenology of the MSSM subject to vanishing scalar soft terms. We generalize our study by including non-vanishing Higgs boson soft masses, as well as a Higgs boson bilinear B term. This does not reintroduce a flavor problem. Inspired by grand-unified theories, we take our input scale to be M_{GUT} , and demand universal gaugino masses at this scale.¹ After imposing consistent electroweak symmetry breaking, the independent parameters of this theory, which we call Higgs Exempt No-Scale (HENS) supersymmetry, are

$$M_{1/2}, \quad \tan \beta, \quad m_{H_u}^2, \quad m_{H_d}^2, \quad \text{sgn}(\mu), \quad (1)$$

where $M_{1/2}$ is the universal gaugino mass at M_{GUT} , $\tan \beta$ is the ratio of the Higgs boson expectation values, $m_{H_u}^2$ and $m_{H_d}^2$ are the soft Higgs masses at M_{GUT} , and $\text{sgn}(\mu)$ is the sign of the supersymmetric Higgs bilinear μ term.

The outline of this paper is as follows. In Section 2 we motivate this scenario, and show how it can emerge in a number of different ways. Section 3 discusses the low-energy mass spectrum of the model, the acceptable regions of parameter space, and the most important constraints on these regions. In Section 4 we investigate the prospects for dark matter in the model, and discuss some of the potential signatures this might induce. Section 5 contains an investigation of some of the potential collider signatures of the model at the Tevatron and the LHC, as well as a discussion of the discovery prospects at these machines. Finally, Section 6 is reserved for our conclusions.

While this work was in preparation, we became aware of Refs. [20, 22], which investigate the mass spectrum and dark matter prospects of gaugino mediation with unsuppressed Higgs soft masses. There is some overlap between their work and the material in Sections 3 and 4 of this paper. However, unlike Refs [20, 22], we allow negative Higgs soft squared masses at the input scale [23], and have a more extensive discussion of the phenomenological constraints. On the other hand, they consider specific details of gaugino mediated models, and discuss the possibility of gravitino dark matter in more detail than we do.

¹For the case of non-universal gaugino masses but vanishing Higgs soft terms, see [21].

2 Generating Small Scalar Soft Terms

Our primary motivation for considering models with small scalar soft terms is data driven: they provide a simple and elegant reason for small flavor violations induced by supersymmetry. Even so, it is comforting that this framework can arise from a number of theoretical constructions. In this section we describe some of these models, and discuss how they can be modified to allow for non-vanishing soft masses for the Higgs fields.

2.1 Models

Vanishing scalar soft terms have traditionally been associated with no-scale models [15]. These models are attractive because the gravitino mass, and therefore the scale of supersymmetry breaking, is determined dynamically. The basic assumption underlying no-scale constructions is that the effective superspace Kähler density and superpotential have the form [24, 25, 26, 27]

$$\begin{aligned}\mathcal{F} &= -3 M_{\text{Pl}}^2 + f(X) + f^\dagger(X^\dagger) + g(\Phi, \Phi^\dagger), \\ \mathcal{W} &= W(\Phi),\end{aligned}\tag{2}$$

where X is a hidden sector field, Φ represents a visible sector field, and W is a holomorphic cubic function. With this form of the Kähler density and superpotential, the tree-level potential along the direction of the hidden sector field X is flat, the gravitino mass, $m_{3/2}$ is undetermined, and no soft terms are generated for the visible sector scalars. Supersymmetry breaking is communicated to the visible sector by non-trivial X -dependent gauge kinetic functions, which generate gaugino soft masses on the order of $m_{3/2}$. The one-loop corrections from the gauginos lift the potential in the X direction and fix the value of $m_{3/2}$ to lie close to the electroweak scale, which is determined dynamically by the large top Yukawa coupling [25].

It is difficult to maintain $m_{3/2} \sim M_W$ in no-scale models if there are other larger scales in the theory because of the radiative corrections these contribute to the effective potential for $m_{3/2}$ [27]. If such large scales exist, such as in a GUT, the heavy sector must be completely sequestered from the supersymmetry breaking, since in the supersymmetric limit, they do not alter the effective potential. Within a GUT where the Higgs superfields are components of complete multiplets that also contain heavy fields, it is therefore essential to prevent these GUT multiplets from obtaining a supersymmetry breaking mass. Having separated the Higgs in this way, it is natural to sequester the other chiral multiplets as well. This is the origin of the vanishing scalar soft terms in no-scale models. Gaugino masses can be induced by a non-minimal kinetic function for those and only those components of the GUT vector multiplet that remain light. Thus if the Higgs multiplets are components of a larger GUT multiplet, of which some components develop GUT scale masses, it is not possible to generate soft masses for the Higgs fields without destabilizing $m_{3/2}$. On the other hand, soft Higgs masses might be possible in more general unification scenarios in which the Higgs fields do not belong to complete GUT multiplets [28].

The form of the no-scale Kähler density and superpotential, Eq. (2), is an input to these models. Such a form does arise to lowest order in several string- and M-theory constructions,

but is typically corrected at higher orders [29]. More generally, a superspace Kähler density in which the visible and hidden sectors appear as disjoint terms, as in Eq. (2), is said to be *sequestered* [9]. A sequestered Kähler density and superpotential guarantees that no direct soft terms are generated. This is a necessary ingredient for anomaly mediation [9].

Complete sequestering can be obtained geometrically by confining the visible and hidden sectors to branes separated by an extra-dimensional bulk [9]. A partial sequestration can also be realized if the MSSM gauge multiplets are allowed to propagate in the bulk, as in gaugino mediated supersymmetry breaking [14]. If so, the gauginos will develop soft masses through their local couplings to the hidden sector, while the soft terms of the chiral multiplets will only be generated by loops passing across the bulk. The resulting supersymmetric spectrum at the compactification scale of the extra dimension is therefore close to the one we are interested in: non-zero gaugino masses, and much smaller soft scalar terms. By allowing the Higgs multiplets to propagate in the bulk, non-zero Higgs soft terms can be generated as well. This is perhaps the simplest way to realize the HENS models we shall consider.

Sequestering can also be realized in four dimensions through strongly-coupled conformal dynamics in the hidden sector [16]. Even without strong conformal running, the contributions to the gaugino masses and the trilinear A are naturally suppressed relative to the gravitino mass if there are no singlets in the hidden sector. This is not true for the scalar soft masses, which are generated by terms like

$$\mathcal{L} \supset \int d^4\theta \frac{c_{ij}}{M_*} \Phi_i^\dagger \Phi_j X^\dagger X \rightarrow \frac{c_{ij} |F_X|^2}{M_*} \phi_i^* \phi_j, \quad (3)$$

where M_* is the messenger scale, X is a hidden sector field, and Φ_i is a visible field. Operators of the form of Eq. (3) can be suppressed relative to the gravitino mass by strong conformal dynamics in the hidden sector that couples at the renormalizable level to X [30]. If all such soft mass contributions are sufficiently suppressed,² and if there are no hidden sector singlets, the visible sector is sequestered and the leading contribution to the soft terms comes from anomaly mediation. By allowing singlets in the hidden sector, both gaugino masses and A terms can be generated that are much larger than the anomaly-mediated terms [30]. This is close to, but not quite, the spectrum we are interested in, because it is unclear how to avoid suppressing the Higgs soft masses while squashing the rest.

A partial sequestration of soft terms, as well as an explanation for the Yukawa hierarchy, can also be obtained from strong conformal dynamics in the visible sector [31, 32, 33]. In these constructions, there is a new gauge group G_c that approaches a strongly-coupled fixed point in the IR. The MSSM fields are not charged under G_c , but they do couple to fields that are through cubic operators in the superpotential. As the theory flows towards the fixed point, the MSSM fields develop large anomalous dimensions which suppress their corresponding (physical) Yukawa couplings. Since different (linear combinations of) fields develop distinct anomalous dimensions, related to their effective superconformal R charges, a Yukawa hierarchy can be generated in this way [31]. The conformal running also produces

² All the soft masses will be suppressed provided there are no unbroken, non-anomalous global symmetries in the hidden sector. The amount of suppression depends on the range over which the conformal running takes place and the beta-function of the corresponding gauge coupling.

a general suppression of the soft scalar masses, as well as a hierarchy of trilinear A terms that mirrors the Yukawa couplings [31, 32, 33, 34]. Conversely, the gaugino masses are largely unaffected because they do not couple directly to the strongly-coupled sector. The third generation multiplets and the Higgs multiplets must also be shielded from the conformal running effects to avoid suppressing the top quark Yukawa coupling. As a result, the third generation and the Higgs soft masses do not get suppressed. Thus, the spectrum from visible sector conformal running is similar to one we shall consider, but augmented by third generation soft masses and A terms.³ We expect the phenomenology of both scenarios to be similar over much of the allowed parameter space.

2.2 The Scale of M_c

From the discussion above, we see that a HENS soft mass spectrum can arise from gaugino mediation with the Higgs multiplets in the bulk, or from conformal running in the hidden sector up to additional contributions to the third generation states. Before proceeding, however, let us comment on our choice of M_{GUT} as the input scale for the soft spectrum. In gaugino mediation, the input scale is on the order of the compactification scale, M_c .⁴ For visible-sector conformal running, the input scale for the soft spectrum is the scale at which the conformal running ceases, which we will also call M_c . Our motivation to set $M_c = M_{GUT}$ is partly conventional, but is also motivated by gauge unification and our wish to strongly suppress the scalar soft masses.

In both cases, gauge unification can be preserved with $M_c < M_{GUT} \sim 2 \times 10^{16}$ GeV, but the process will be more complicated than in the standard picture. In gaugino mediation, Kaluza-Klein states appear above M_c and can lead to an accelerated power-law running [35]. With conformal dynamics in the visible sector, the SM gauge coupling beta functions will be modified by the large anomalous dimensions of the MSSM fields. Gauge unification will still occur, albeit at a lower scale, provided the conformal dynamics respects a global symmetry into which the SM gauge group can be embedded [36]. Thus, in each case having M_c below M_{GUT} can induce an effective unification of the SM gauge couplings below the apparent unification scale $M_{GUT} \simeq 2 \times 10^{16}$ GeV. This is problematic for many GUT completions of the MSSM, which predict baryon and lepton number violation. Typically, some additional structure is needed if M_c is much smaller than M_{GUT} . This motivates us to consider $M_c \geq M_{GUT}$.

It is clear that gauge unification can also be maintained with $M_c \geq M_{GUT}$. If M_c is larger than M_{GUT} , the renormalization group running from M_c down to M_{GUT} will induce non-vanishing (flavor-universal) soft masses at M_{GUT} . The size of these corrections from running above M_{GUT} depends on the precise GUT completion of the theory, but even for

³There may also be additional contributions to the soft masses if there are non-anomalous, continuous, abelian global symmetries.

⁴ $M_c := 1/R$, is less than the cutoff of the theory.

minimal GUT models they can be significant, on the order of [17, 18]

$$\begin{aligned}\Delta A &\simeq \frac{2\alpha_G}{\pi} C_A \ln\left(\frac{M_c}{M_{GUT}}\right) M_{1/2}, \\ \Delta m^2 &\simeq \frac{2\alpha_G}{\pi} C_{m^2} \ln\left(\frac{M_c}{M_{GUT}}\right) M_{1/2}^2,\end{aligned}\tag{4}$$

where $\alpha_G \simeq 1/24$ is the GUT coupling, and C_A and C_{m^2} are dimensionless constants on the order of or slightly larger than unity. These contributions can be large enough for an acceptable low-energy spectrum to be obtained [17, 18].

On the other hand, in both gaugino mediation and conformal sequestering, M_c cannot be more than about an order of magnitude above M_{GUT} because the suppression of soft terms (and Yukawa couplings) requires a separation of scales. Let M_{in} be the scale at which conformal running begins in the case of conformal dynamics, or the UV cutoff of the extra-dimensional gauge theory in gaugino mediation. Presumably $M_{in} \leq M_{P1} = 2.4 \times 10^{18}$ GeV. The amount of suppression of the soft scalar terms from conformal running is expected to be an order-one power of M_c/M_{in} , whereas the required suppression is typically on the order of 10^{-4} [32]. An even stronger upper bound on M_c can be obtained if the conformal dynamics are responsible for the small electron Yukawa coupling as in Ref. [31]. The condition for this is

$$y_e \simeq \left(\frac{3 \times 10^{-6}}{\cos \beta}\right) \simeq \left(\frac{M_c}{M_{in}}\right)^{(\gamma_L + \gamma_E)/2},\tag{5}$$

where γ_i denote the anomalous dimensions of L and E^c , which are generally smaller than 2. If we take this bound seriously, M_c can be at most only slightly larger than M_{GUT} . In gaugino mediation, flavor-mixing contact interactions between the MSSM chiral multiplets and hidden sector operators, arising from bulk states with masses above the UV cutoff scale, are suppressed by a factor of $\exp(-M_{in}/M_c)$ [14]. Again this factor must be less than about 10^{-4} to avoid various experimental flavor constraints, which translates into M_c being within an order of magnitude larger than M_{GUT} (for $M_{in} = M_{P1}$).

Given the above considerations, we will set $M_c = M_{GUT}$ throughout this paper, and not concern ourselves with the precise mechanism by which the scalar soft terms are suppressed. While beyond the scope of the present work, it is also interesting to speculate that the breaking of the GUT symmetry is related to the geometry of the extra dimension, or the escape from conformal running. Such a construction would further justify our choice of $M_c = M_{GUT}$. Finally, let us also note that within particular models there is typically some residual flavor violation due to an incomplete suppression of the scalar terms at M_c . The amount of flavor suppression can be close to the level probed by current experiments. However, without specifying a particular model, it is not possible to perform an analysis of the constraints due to flavor physics. Thus, we assume as our starting point that at the scale $M_c = M_{GUT}$, all scalar masses except those of the Higgs bosons are precisely zero and that corrections to that assumption are inconsequential to the phenomenology discussed below.

3 Mass Spectrum and Constraints

3.1 One-Loop Analysis

The essential features of the HENS mass spectrum are well illustrated by a simple one-loop analysis. At this order, the ratio M_a/g_a^2 , $a = 1, 2, 3$, is scale invariant for all three gaugino masses. If the gauge couplings unify and the gaugino masses are universal at M_{GUT} , it follows that at lower scales Q , $M_a(Q) = [g_a(Q)/g_{GUT}]^2 M_{1/2}$. For $Q = 1$ TeV, this gives

$$M_1 \simeq (0.43) M_{1/2}, \quad M_2 \simeq (0.83) M_{1/2}, \quad M_3 \simeq (2.6) M_{1/2}. \quad (6)$$

The one-loop running of the scalar soft masses is given by [1, 37]

$$(4\pi)^2 \frac{dm_i^2}{dt} \simeq X_i - 8 \sum_a C_i^a g_a^2 |M_a|^2 + \frac{6}{5} g_1^2 Y_i S, \quad (7)$$

where X_i depends on the soft masses and A terms and is usually proportional to Yukawa couplings, C_i^a is the quadratic Casimir for the representation i under gauge group a , and

$$S = (m_{H_u}^2 - m_{H_d}^2) + tr_F(m_Q^2 - 2m_U^2 + m_E^2 + m_D^2 - m_L^2), \quad (8)$$

with the trace above running over flavors.

At one-loop order, the RG equation for the S term is particularly simple,

$$(4\pi)^2 \frac{dS}{dt} = \frac{66}{5} g_1^2 S. \quad (9)$$

Because of this simple form, the effect of the S -term on the low-scale soft masses is to simply shift the value they would have with $S = 0$ by the amount

$$\Delta m_i^2 = -\frac{Y_i}{11} \left[1 - \left(\frac{g_1}{g_{GUT}} \right)^2 \right] S_{GUT} \simeq -(0.052) Y_i S_{GUT}, \quad (10)$$

where $S_{GUT} = (m_{H_u}^2 - m_{H_d}^2)$ evaluated at M_{GUT} .

Neglecting Yukawa effects, the low-scale slepton soft masses at $Q = 1$ TeV are

$$m_L^2 \simeq [(0.68) M_{1/2}]^2 + \frac{1}{2} (0.052) S_{GUT}, \quad (11)$$

$$m_E^2 \simeq [(0.39) M_{1/2}]^2 - (0.052) S_{GUT}. \quad (12)$$

If mixing effects are small, the physical slepton masses will be close to $\sqrt{m_L^2}$ and $\sqrt{m_E^2}$, up to the $U(1)_Y$ D -term contributions. The mass of the lightest neutralino is usually close to M_1 (under the assumption of gaugino universality) unless μ is relatively small.

Comparing Eq. (11) with Eq. (6), we see that for $S_{GUT} \geq 0$, m_E^2 is less than M_1 and the lightest superpartner tends to be a mostly right-handed slepton. On the other hand, if $S_{GUT} < 0$, the right-handed slepton soft mass is pushed up relative to M_1 , allowing for a mostly Bino neutralino LSP. For S_{GUT} very large and negative, the LSP can be a mostly left-handed slepton. Relative to the sleptons and the electroweak gauginos, the squarks and gluino are very heavy because the $SU(3)_c$ gauge coupling grows large in the infrared.

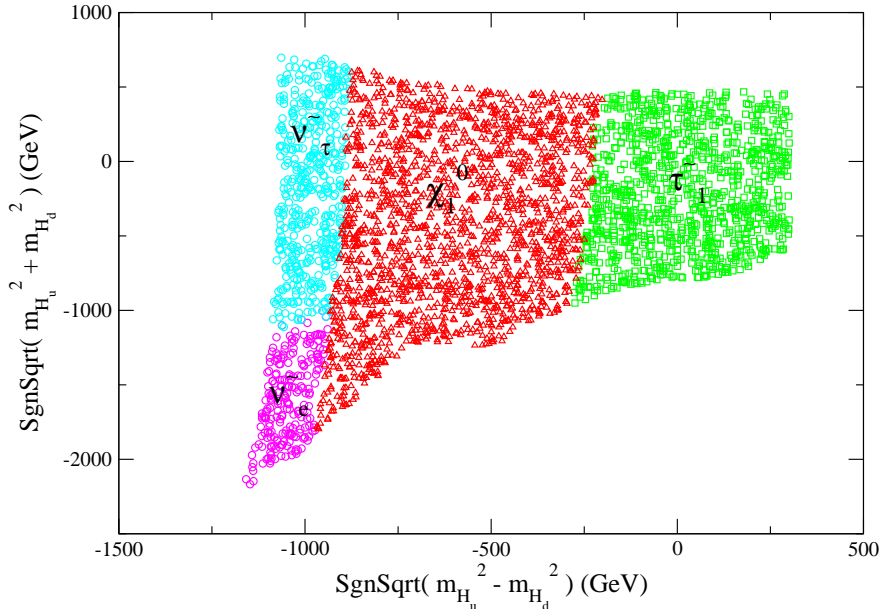


Figure 1: Allowed parameter regions for $\tan\beta = 10$ and $M_{1/2} = 300$ GeV. The differently colored regions in the figure indicate the identity of the lightest superpartner. The quantities $m_{H_u}^2$ and $m_{H_d}^2$ are evaluated at the input scale M_{GUT} .

3.2 Parameter Space Scans

To confirm the simple analysis given above, we have performed a scan over the HENS parameter space using SuSpect 2.34 [38]. This code performs the renormalization group running at two-loop order with one-loop threshold effects, and includes radiative and mixing corrections to the physical particle masses. We take $\alpha_s(M_Z) = 0.118$ [39] and $m_t = 171.4$ GeV [40] in our analysis. For each model parameter point we require consistent electroweak symmetry breaking, and superpartner masses above the LEP II and Tevatron bounds ($m_{\chi_1^0}, m_{\tilde{\nu}} > 46$ GeV, $m_{\tilde{t}} > 90$ GeV, $m_{\chi_1^\pm} > 104$ GeV). We also impose the lower-energy constraints

$$\begin{aligned} \Delta\rho &\in [-8, 24] \times 10^{-4} & [39] \\ BR(b \rightarrow s\gamma) &\in [3.0, 4.0] \times 10^{-4} & [41] \\ \Delta a_\mu &\in [-5, 50] \times 10^{-10} & [39] \end{aligned} \tag{13}$$

These ranges correspond approximately to the 95% *c.l.* allowed values, although we have allowed a slightly larger range for Δa_μ . The constraint from the muon magnetic moment is particularly interesting in HENS scenarios, and we shall discuss it more extensively below. In the immediate analysis we do not include the LEP II bound on the lightest Higgs boson mass. We will discuss this constraint below as well.

Figures 1, 2, and 3 show the allowed regions of $m_{H_u}^2(M_{GUT})$ and $m_{H_d}^2(M_{GUT})$, for $(\tan\beta, M_{1/2})$ equal to $(10, 300$ GeV), $(10, 500$ GeV), and $(30, 500$ GeV), subject to the

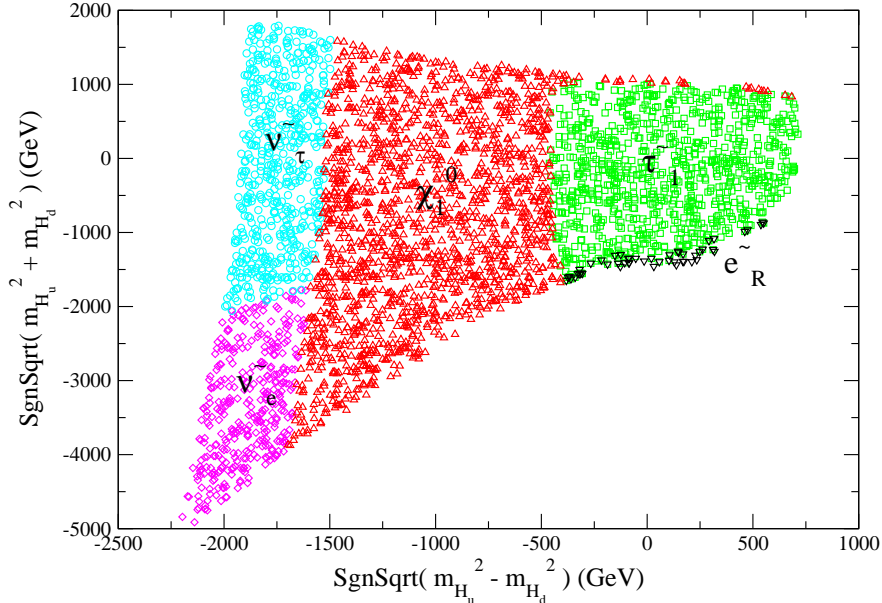


Figure 2: Allowed parameter regions for $\tan\beta = 10$ and $M_{1/2} = 500$ GeV. The differently colored regions in the figure indicate the identity of the lightest superpartner. The quantities $m_{H_u}^2$ and $m_{H_d}^2$ are evaluated at the input scale M_{GUT} .

constraints described above. The soft Higgs masses in these plots are re-expressed in terms of the more convenient combinations $SgnSqrt(m_{H_u}^2 - m_{H_d}^2)(M_{GUT}) = S_{GUT}/\sqrt{|S_{GUT}|}$, and $SgnSqrt(m_{H_u}^2 + m_{H_d}^2)(M_{GUT})$, where $SgnSqrt$ denotes the signed square root ($SgnSqrt(\pm x^2) = \pm x$). Also shown in these plots is the identity of the lightest superpartner at each allowed parameter point.

These figures confirm our previous approximate analysis. When S_{GUT} is positive or zero, the LSP is a mostly right-handed stau or selectron. As S_{GUT} becomes more negative, a neutralino becomes the LSP, while for very large and negative values of S_{GUT} the LSP is a sneutrino. For extremely large positive or negative values of S_{GUT} , one of the slepton soft masses becomes tachyonic. The allowed parameter region is cut off at larger positive values of $(m_{H_u}^2 + m_{H_d}^2)(M_{GUT})$ because $|\mu|^2$ only has a negative solution, implying that electroweak symmetry breaking is not possible.⁵ Note that in Fig. 2, there is a thin strip along the upper border of the allowed region in which the LSP is a neutralino. In this strip, the μ term is smaller than M_1 and the neutralino LSP is mostly Higgsino. For larger negative values of $(m_{H_u}^2 + m_{H_d}^2)(M_{GUT})$, $M_{A^0}^2 \rightarrow 0$ and the parameter space gets cut off by the bound from $BR(b \rightarrow s\gamma)$. As $(m_{H_u}^2 + m_{H_d}^2)(M_{GUT})$ becomes even smaller, electroweak symmetry breaking ceases to occur.

The effects of the τ Yukawa coupling and left-right mixing can be seen by comparing

⁵In fact, the parameter space is cut before μ reaches zero by the $BR(b \rightarrow s\gamma)$ and the chargino mass constraints.

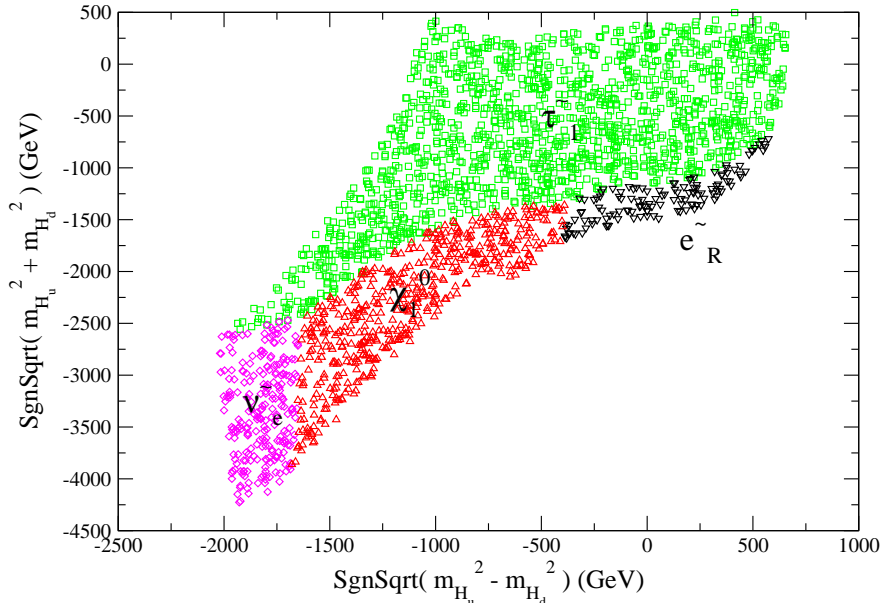


Figure 3: Allowed parameter regions for $\tan\beta = 30$ and $M_{1/2} = 500$ GeV. The differently colored regions in the figure indicate the identity of the lightest superpartner. The quantities $m_{H_u}^2$ and $m_{H_d}^2$ are evaluated at the input scale M_{GUT} .

Figs. 2 and 3. In the models we are considering, the value of the Yukawa-dependent term in Eq. (7) for the right-handed stau soft mass is

$$X_{E_3} \simeq 2|y_\tau|^2 m_{H_d}^2. \quad (14)$$

The left-right mixing is also proportional to the τ Yukawa. As $\tan\beta$ increases, so too does the τ Yukawa, and therefore also the Yukawa effect on the running and the mixing. Left-right mixing tends to push the lighter stau mass lower, and for this reason it is more difficult to obtain a neutralino LSP at larger values of $\tan\beta$. However, there is also a competing effect from the influence of the τ Yukawa on the running of $m_{E_3}^2$. When $m_{H_d}^2$ is large and negative, the X_{E_3} term increases the value of $m_{E_3}^2$ at low energies. Thus, a selectron or an electron sneutrino is the LSP in some parts of the parameter space.

In parts of the parameter space shown in Figs. 1-3 the value of $m_{H_u}^2$ is large and negative, while the slepton soft masses are considerably smaller in magnitude (but positive). In these regions, it is likely that the standard MSSM minimum is only metastable, and that a deeper charge-breaking minimum exists at large field values [42]. The precise constraints on the existence of such non-standard global minima depend on the details of the thermal history of the Universe [43], and we do not investigate them in the present work. However, a necessary condition is that the lifetime of the metastable MSSM vacuum at $T = 0$ should be greater than the age of the universe. While beyond the scope of the present work, it is possible that some regions of the parameter space shown in Figs. 1-3, especially the lower left region and at larger values of $\tan\beta$, may not be populated after a more detailed analysis.

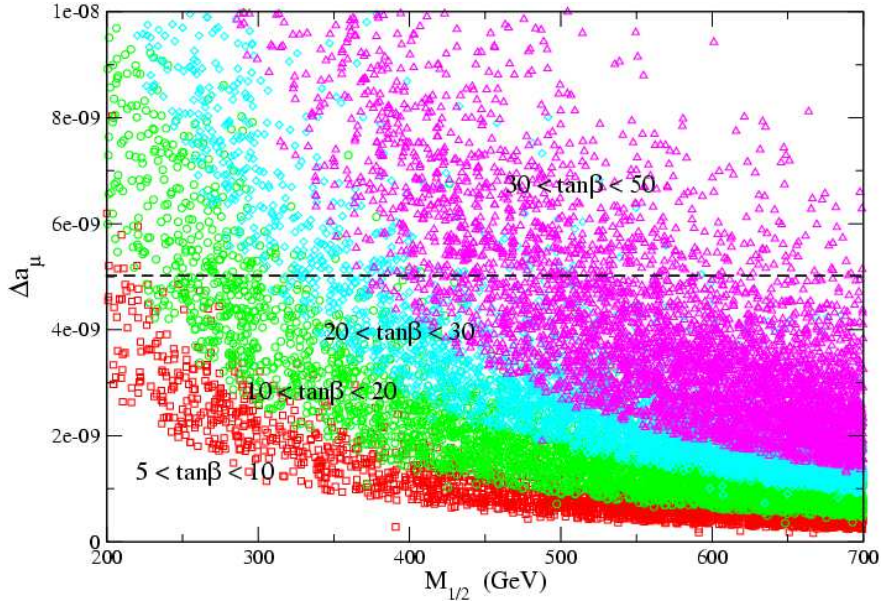


Figure 4: Δa_μ^{SU5Y} as a function of $M_{1/2}$ for several ranges of $\tan\beta$, and $sgn(\mu) > 0$. The spread of points come from scanning over the acceptable input values of $m_{H_u}^2$ and $m_{H_d}^2$. The red points indicate $\tan\beta \in [5, 10)$, the green points $\tan\beta \in [10, 20)$, the blue points $\tan\beta \in [20, 30)$, and the magenta points $\tan\beta \in [30, 50)$.

3.3 Constraints from $(g-2)_\mu$

Since the sleptons in HENS models are relatively light, the corrections to the anomalous magnetic moment of the muon, $a_\mu = (g-2)_\mu/2$ can be significant [44]. Currently, the measured value of a_μ exceeds the SM prediction by about two standard deviations [39],

$$\Delta a_\mu = a_\mu^{exp} - a_\mu^{SM} = (22 \pm 10) \times 10^{-10}. \quad (15)$$

This result is suggestive of new physics.

In the MSSM, there are additional contributions to $(g-2)_\mu$ from loops involving a virtual chargino and muon sneutrino, and loops with a virtual neutralino and smuon. For the HENS scenarios we are studying, in which all masses scale predominantly with $M_{1/2}$ and the gaugino masses are universal (and assumed real and positive), the leading supersymmetry contribution to a_μ is proportional to $\tan\beta$, scales roughly as $M_{1/2}^{-2}$, and has a sign equal to the sign of the μ term, $sgn(\mu)$ [45]. Given the tension between the measured value of Δa_μ and the SM prediction, $sgn(\mu) > 0$ is strongly favored. Indeed, we find that negative $sgn(\mu)$ is only possible for very large values of $M_{1/2}$. Conversely, if $sgn(\mu)$ is positive the new supersymmetric contribution can help to explain this possible discrepancy between the SM prediction and experiment.

The value of Δa_μ^{SU5Y} is shown as a function of $M_{1/2}$ in Fig. 4. In generating this figure, we have taken $sgn(\mu) > 0$, and have scanned over input values of $m_{H_u}^2$ and $m_{H_d}^2$ at M_{GUT} .

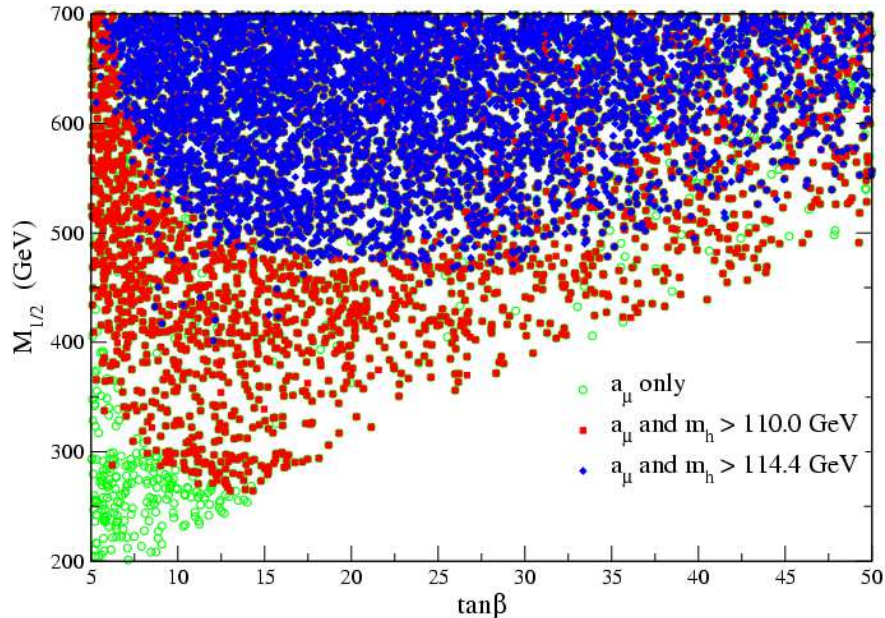


Figure 5: Scatter plot in the $M_{1/2} - \tan\beta$ plane of solutions that respect the bounds of $\Delta a_\mu^{SUSY} < 50 \times 10^{-10}$ and $m_h > 114.4$ GeV. Due to uncertainty in the top quark mass, and the theoretical uncertainty in the computation of m_h , a more conservative constraint on this theoretically computed value of m_h is 110 GeV, which is also shown in the figure.

The distribution for $sgn(\mu) < 0$ looks the same, except the sign of Δa_μ is opposite. With $sgn(\mu) > 0$, the new physics contribution is frequently too large, and from this we obtain a lower bound on $M_{1/2}$ as a function of $\tan\beta$. For $\tan\beta = 10$, this bound is $M_{1/2} \gtrsim 250$ GeV, while for $\tan\beta = 30$, it increases to $M_{1/2} \gtrsim 400$ GeV.

3.4 Constraints from the Higgs Boson Mass

A further constraint on HENS models, and one we have not yet imposed, is that the SM Higgs boson mass should exceed the LEP II bound [46],

$$m_h > 114.4 \text{ GeV}. \quad (16)$$

This bound also applies to the lightest CP-even Higgs boson in much of the parameter space of the MSSM. However at tree-level in the MSSM, the lightest CP-even Higgs boson has a mass below M_Z . It is only because of large loop corrections to the mass, predominantly due to the scalar tops, that this Higgs state can be raised above the LEP II bound. With vanishing input scalar soft masses, the stop masses scale with $M_{1/2}$. The Higgs boson mass bound therefore imposes a further lower bound on the universal input gaugino mass.⁶

⁶One could increase the Higgs mass by introducing a SM singlet Higgs field to the spectrum, but this introduces tensions with grand unification [47].

The combined bounds on $M_{1/2}$ as a function of $\tan\beta$ from the conditions $\Delta a_\mu < 50 \times 10^{-10}$ and $m_h > 110.0$ (114.4) GeV are shown in Fig. 5. We impose a slightly weaker 110 GeV lower bound on the Higgs boson mass than the 114 GeV LEP II bound to account for various uncertainties associated with the theoretical computation of m_h . We have taken $m_t = 171.4$ GeV in our analysis. At smaller $\tan\beta$, less than about 15, the Higgs mass bound imposes the stronger constraint, while the upper bound on Δa_μ is more significant for values of $\tan\beta > 15$. For any value of $\tan\beta$, $M_{1/2}$ must be greater than about 300 GeV if we impose the weaker Higgs mass bound ($m_h > 110.0$ GeV), and larger than about 500 GeV to satisfy the stronger bound ($m_h > 114.4$ GeV). Note that as $M_{1/2}$ grows, the phenomenological constraints on the model tend to weaken, but usually at the cost of increased fine-tuning in the Higgs sector [48].

4 Dark Matter and Cosmological Signals

In the previous section, we found that in a large region of the HENS parameter space a slepton or a sneutrino is the LSP. Such an LSP can be problematic for cosmology. If the LSP is a charged slepton, the very strong constraints that exist for charged stable particles imply that such a scenario is all but ruled out [49]. These bounds do not apply to a sneutrino LSP, but in this case the direct detection rate is much too high (for a mass of ~ 100 GeV) [50]. Without invoking some additional and interesting mechanisms that allow the sneutrino as a more viable LSP [51], we will focus on the case of a neutralino LSP. Also, a slepton as the lightest superpartner particle, charged or not, may still provide a consistent picture of dark matter if the gravitino is the LSP [52]. We will comment briefly on that possibility later.

4.1 Neutralino LSP Relic Density

We investigate the relic density of neutralino LSPs at various points in the allowed parameter space with the aid of DarkSUSY 4.1 [53]. This computer program performs a fully relativistic computation of the relic density, and includes all relevant coannihilation channels.

Figures 6 and 7 show the neutralino LSP relic density for $\tan\beta = 10$, $M_{1/2} = 300$ GeV and 500 GeV, and $\mu > 0$ for the full range of allowed input values of $m_{H_u}^2$ and $m_{H_d}^2$ at $M_c = M_{GUT}$. In both figures the black plus signs indicate the regions in which the lightest neutralino is not the LSP, but that are otherwise allowed. The red triangles correspond to parameter points where the neutralino relic density is acceptably small, $\Omega h^2 < 0.11$. This is to be compared with the observed dark matter density [54],

$$\Omega h^2 = 0.1045_{-0.0095}^{+0.0072} \quad (\text{WMAP only}). \quad (17)$$

In the blue, green, and magenta regions, the neutralino relic density exceeds 0.11. These regions can still be consistent with the WMAP measurements if there is a late-time injection of entropy into the universe after the neutralinos have frozen out [55].

The shape of the neutralino relic density contours in Figs. 6-7 can be understood in terms of the mass spectrum of the model. In most of the parameter space, the lightest neutralino

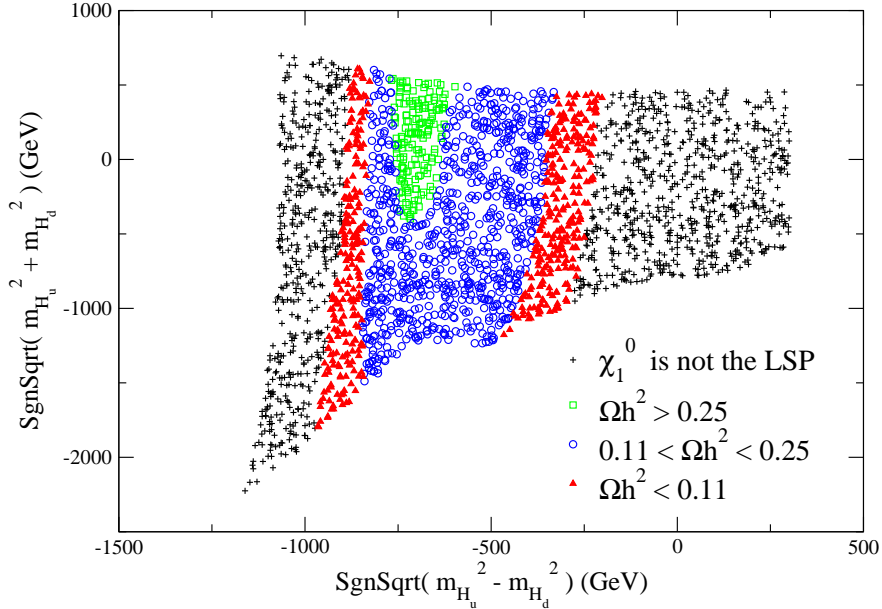


Figure 6: Neutralino LSP relic density for $\tan\beta = 10$, $M_{1/2} = 300$ GeV, and $\text{sgn}(\mu) > 0$. The region in which the lightest neutralino is not the LSP is denoted by the black plus signs. The red triangles indicate parameter points where the neutralino LSP relic density is less than $\Omega h^2 < 0.11$. In the blue and green regions, the neutralino LSP relic density exceeds this value.

is predominantly Bino. The main annihilation channels in this bulk region are t -channel slepton exchanges. This is not efficient enough to reduce the relic density to an acceptable level for the values of $M_{1/2}$ that are relevant, although it does come close for $M_{1/2} = 300$ GeV.

Along the left and right edges of the neutralino region, the mass of the neutralino LSP approaches that of the lightest slepton. This near degeneracy allows for coannihilation between the neutralino LSP and the lightest slepton to become effective, pushing the neutralino relic density to a value well below the WMAP value. Moving away from these edges towards the bulk region, the coannihilation efficiency falls off quickly, roughly as $\exp[-(m_{\tilde{l}} - m_{\chi^0})/T]$, and the neutralino density goes up. In this transitional region, where slepton coannihilation is only moderately efficient, the correct dark matter density is obtained. The strip of low relic density along the top of the neutralino LSP region arises because the μ parameter becomes small. In this strip, the neutralino LSP develops a significant Higgsino component allowing it to annihilate effectively through gauge bosons, and by coannihilation with the lightest chargino.

In the regions where the lightest neutralino is not the lightest SM superpartner (denoted by black plus signs in Figs. 6-7) the lightest superpartner is always a slepton. On the left-hand side of the neutralino region, this particle is either a tau or an electron sneutrino, as illustrated in Figs. 1-3. On the right, the lightest superpartner is a mostly right-handed stau or selectron. The annihilation of sleptons is very efficient in the early universe. If such a

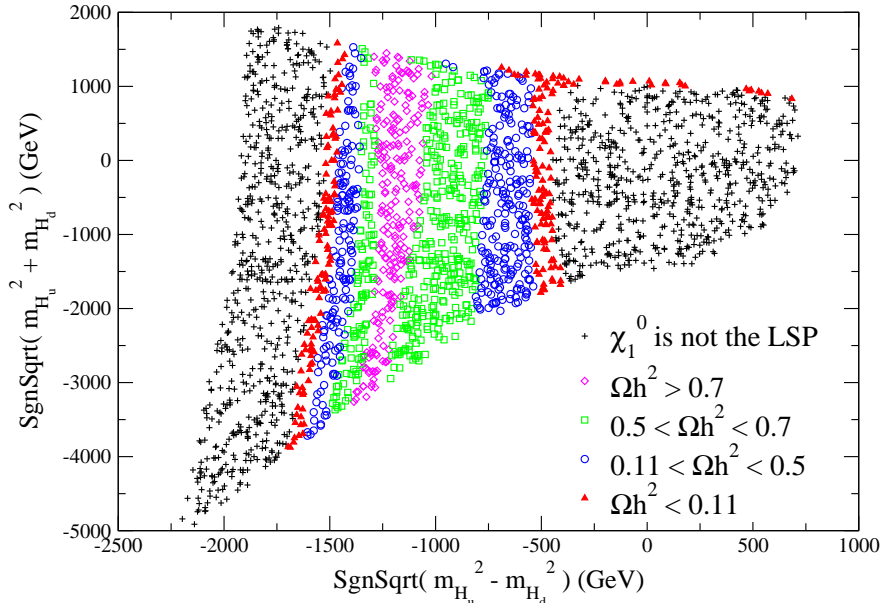


Figure 7: Neutralino LSP relic density for $\tan\beta = 10$, $M_{1/2} = 500$ GeV, and $\text{sgn}(\mu) > 0$. The region in which the lightest neutralino is not the LSP is denoted by the black plus signs. The red triangles indicate parameter points where the neutralino LSP relic density is less than $\Omega h^2 < 0.11$. In the blue, green, and magenta regions, the neutralino LSP relic density exceeds this value.

particle were stable, the relic density in the regions discussed above would be on the order of $\Omega h^2 \sim 10^{-3} - 10^{-2}$. A relic density of heavy charged particles of this size is firmly ruled out by direct searches [49]. Even for a stable sneutrino, a relic density of this size is ruled out by dark matter direct detection searches [56].

A charged or neutral slepton lighter than the lightest neutralino may still be acceptable provided the gravitino is the true LSP. Since the gravitino couples very weakly to the MSSM states, the slepton NLSP would freeze out as if it were the LSP, and decay into gravitinos at a much later time. The final gravitino density produced by these decays is determined by the quasi-stable NLSP density, $\Omega_{\tilde{l}} h^2$, through the relation [52]

$$\Omega_{3/2}^{\text{decay}} h^2 = \frac{m_{3/2}}{m_{\tilde{l}}} \Omega_{\tilde{l}} h^2, \quad (18)$$

where $m_{3/2}$ is the gravitino mass. In the parameter regions we are considering, this density is too small to account for all the dark matter if NLSP decays are the only source of relic gravitinos. However, there are other possible sources of relic gravitinos, such as thermal production after inflationary reheating [57] and non-thermal production through heavy particle decays [58] that can bring the total gravitino relic density up to the value needed to explain all the dark matter. Let us also note that this scenario is constrained by the requirement that the late-time decays not overly disrupt the predictions of big-bang nucleosynthesis or the black-body spectrum of the cosmic microwave background radiation. These constraints

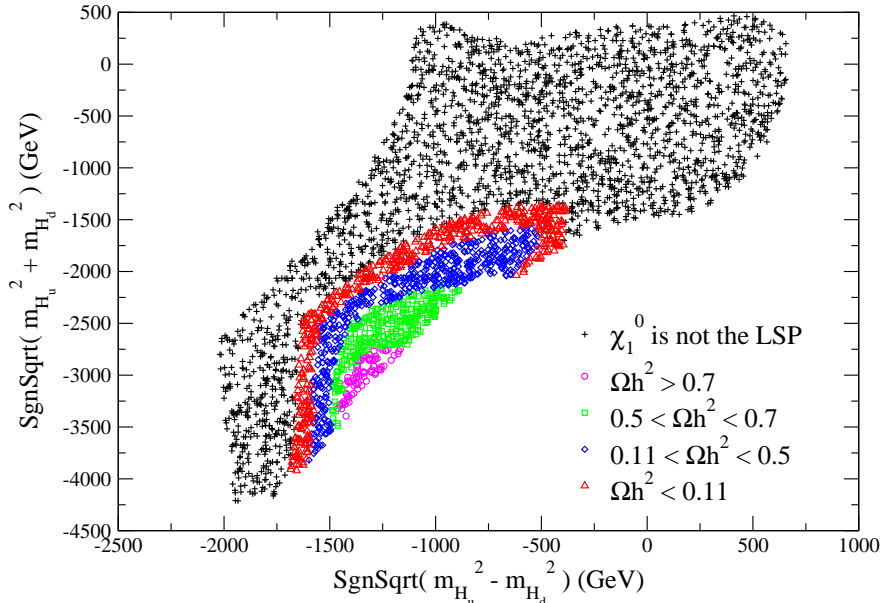


Figure 8: Neutralino LSP relic density for $\tan\beta = 30$, $M_{1/2} = 500$ GeV, and $\text{sgn}(\mu) > 0$. The region in which the lightest neutralino is not the LSP is denoted by the black plus signs. The red triangles indicate parameter points where the neutralino LSP relic density is less than $\Omega h^2 < 0.11$. In the blue, green, and magenta regions, the neutralino LSP relic density exceeds this value.

are relatively weak for a sneutrino NLSP, but they are quite severe for a charged slepton (or neutralino) NLSP, and require $m_{3/2} \lesssim 100$ MeV for most of the range of NLSP masses we are considering [59].

We have also examined the effect of varying $\tan\beta$ on the predictions for dark matter within the model. Smaller values of this ratio, $\tan\beta < 10$, do not change the qualitative features of the picture described above. For $\tan\beta > 10$, there are a couple of important changes. Most importantly, larger values of $\tan\beta$ induce more mixing between the left- and right-handed staus, which has the effect of lowering the mass of the lightest stau. Because of this, for $\tan\beta = 30$ and $M_{1/2} = 500$ GeV there is no longer an acceptable region of parameter space in which the lightest neutralino is both the lightest superpartner, and mostly Higgsino. In Fig. 8 we plot the neutralino LSP relic density for $\tan\beta = 30$, $M_{1/2} = 500$ GeV, and $\text{sgn}(\mu) > 0$. The thin slice of acceptable Ωh^2 arises due to the coannihilation of the LSP with a light slepton.

4.2 Direct and Indirect Detection of Dark Matter

The prospects for direct and indirect detection of neutralino dark matter were investigated using DarkSUSY 4.1 [53]. For the most part, the direct and indirect detection signals within

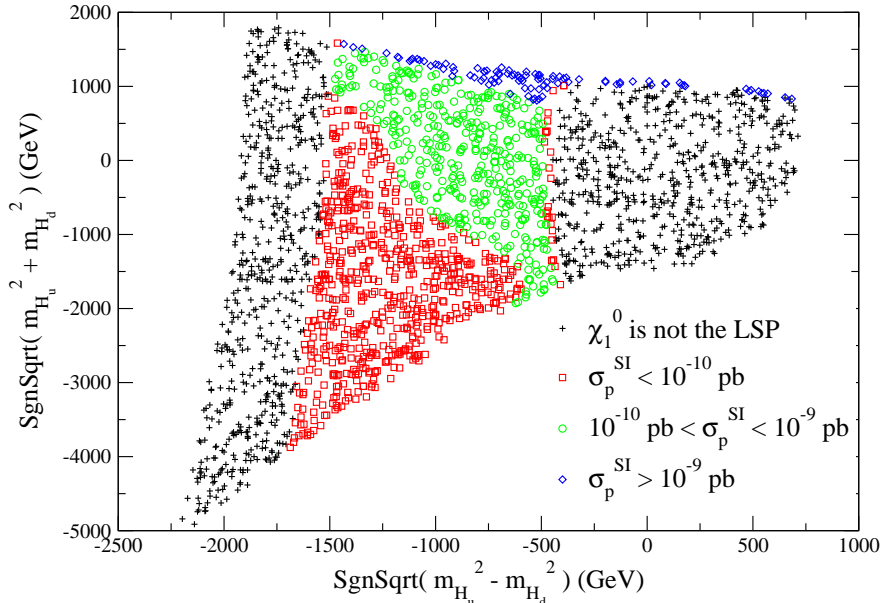


Figure 9: Neutralino-nucleon spin-independent elastic scattering cross section for $\tan \beta = 10$ and $M_{1/2} = 500$ GeV. The black plus signs indicate the parameter region that is consistent with various phenomenological constraints, but need not have a neutralino LSP. The red, green, blue, magenta points indicate parameter points for which a neutralino is the LSP, for several ranges of σ_p^{SI} .

our scenario are very similar to those of a generic mSUGRA model with a mostly Bino LSP [60]. In general, these potential signals are very weak. However, much stronger signals can arise when the neutralino LSP has a significant Higgsino component.

Dark matter in the local halo can be detected directly by its elastic scattering with heavy nuclei. The most strongly constrained neutralino-nucleus cross-sections are the spin-independent ones. It is conventional to express the experimental limits on these cross-sections in terms of an effective neutralino-proton cross-section. The values of the effective spin-independent cross-sections in the present model, for $\tan \beta = 10$ and $M_{1/2} = 500$ GeV, are shown in Fig. 9.⁷ Except in a thin strip at the top of the allowed region, where the neutralino LSP is predominantly Higgsino, these cross-sections are much smaller than the current experimental bound (for a standard set of assumptions about the local halo density) of $\sigma_p^{SI} < 10^{-6} - 10^{-7}$ pb [56] for the range of neutralino masses we consider here. The scattering cross-sections in the Higgsino region are within an order of magnitude this bound.

Spin-independent scattering between a neutralino and a nucleon is mediated predominantly by the exchange of CP-even Higgs bosons and squarks. In the allowed parameter re-

⁷In these figures, the effective cross-section is rescaled by the relic density of the neutralino LSP when it is less than the WMAP value. Such a rescaling is conventional, and accounts for the fact that a smaller density of neutralinos will lead to fewer events in an experiment. This rescaling is also the reason why there is a thin strip with a low effective cross-section on the right-hand side of the allowed region in Fig. 9.

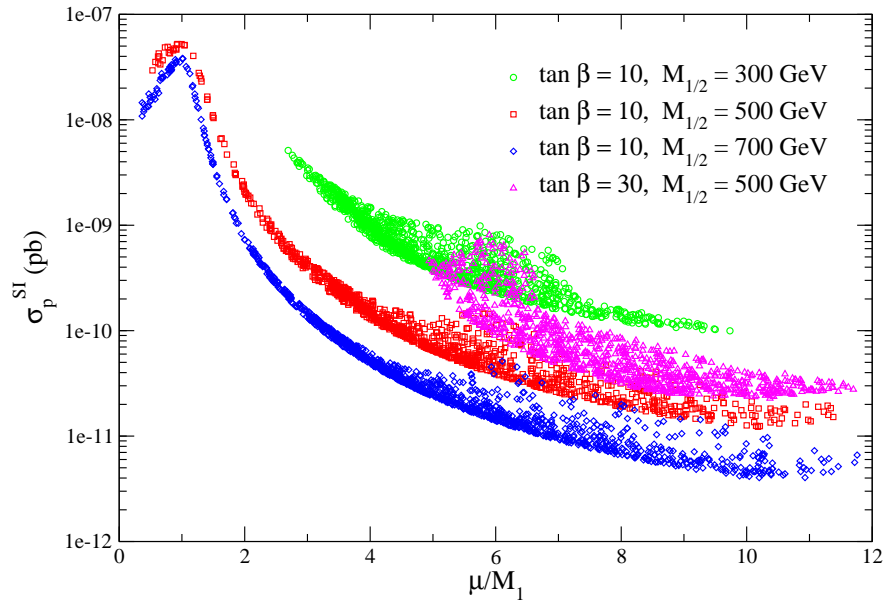


Figure 10: Neutralino-nucleon elastic scattering cross-section for $\tan\beta = 10$ and $M_{1/2} = 300, 500,$ and 700 GeV, as well as for $\tan\beta = 30$ and $M_{1/2} = 500$ GeV, as a function of the ratio μ/M_1 . The current experimental limit for standard assumptions about the local halo density is $\sigma_p^{SI} < 10^{-6} - 10^{-7}$ pb for the range of neutralino masses we consider here [56].

gions discussed above, the squarks tend to be much heavier than the neutralino LSP, thereby suppressing their contribution. Thus, the leading contribution to the spin-independent neutralino-nucleon cross-section usually comes from CP-even Higgs exchange. Since the neutralino Higgs vertices are proportional to the Higgsino component of the neutralino, the effective cross-section depends sensitively on the ratio μ/M_1 . This is illustrated in Fig. 10 for $\tan\beta = 10$ and $M_{1/2} = 300, 500, 700$ GeV, as well as for $\tan\beta = 30$ and $M_{1/2} = 500$ GeV. The dependence on other parameters such as M_{A^0} and $m_{\tilde{q}}$ is much weaker.

Relic neutralinos can also be searched for indirectly by looking for their annihilation products in regions where they tend to clump, and have a local density much larger than the average value. In these particularly dense patches, the rate of neutralino annihilation can become large enough that their products are potentially observable. The most stringent of these indirect detection constraints on neutralino dark matter usually comes from their annihilation in the core of the sun and the earth.⁸ The neutrinos produced by this process can lead to a signal, in the form of a muon flux, in neutrino telescopes.

The best current bound on such a muon flux comes from the Super-Kamiokande experiment [61], and is on the order of $\Phi_\mu \lesssim 10^3 \text{ km}^{-2} \text{ yr}^{-1}$. This sensitivity or bound is expected to be tightened to $10^1 - 10^2 \text{ km}^{-2} \text{ yr}^{-1}$ in the next few years by IceCube [62] and

⁸The rates for other indirect dark matter signals, such as from positron emission, seem to be quite small except when the neutralino LSP is mostly Higgsino, or if the annihilation cross section is enhanced by a s -channel CP-odd Higgs resonance.

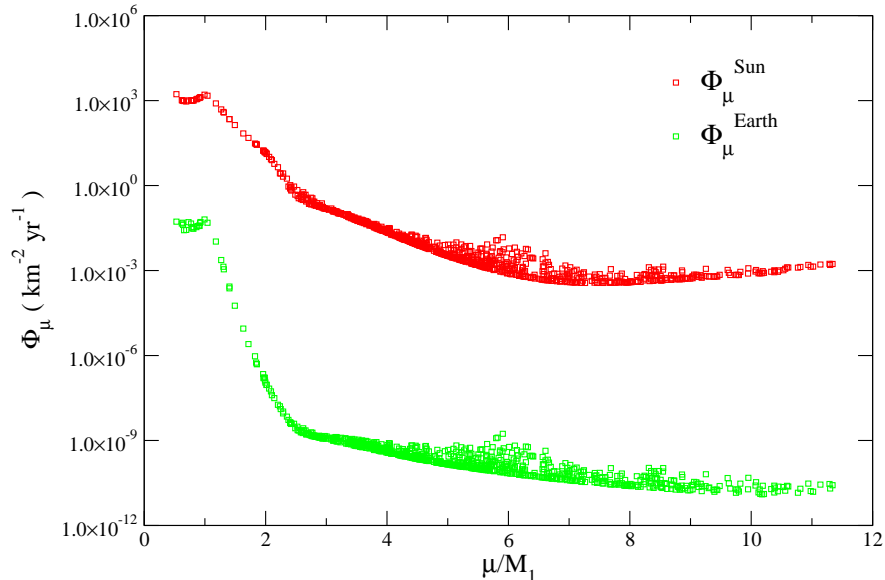


Figure 11: Net muon flux induced by neutralino dark matter annihilation in the core of the sun (red circles) and the Earth (green squares) for $\tan\beta = 10$ and $M_{1/2} = 500$ GeV. A detector threshold of 1 GeV is assumed. The best current bound is $\Phi_\mu \lesssim 10^3 \text{ km}^{-2} \text{ yr}^{-1}$ coming from Super-Kamiokande [61]. Future sensitivities from IceCube and ANTARES are $\Phi_\mu = 10^1 - 10^2 \text{ km}^{-2} \text{ yr}^{-1}$.

ANTARES [63]. The values of Φ_μ due to annihilation in both the core of the earth and the sun in the present model with $\tan\beta = 10$ and $M_{1/2} = 500$ GeV are shown in Fig. 11 as a function of the ratio μ/M_1 , assuming a detector threshold of 1 GeV. As for the direct detection signal, the largest indirect detection signal is obtained when μ/M_1 is on the order of unity and the neutralino LSP has a significant Higgsino component. In fact, for $\mu/M_1 \sim 1$, the signal is at or slightly above the Super-Kamiokande bound. For larger values of μ/M_1 the signal falls off very quickly to values that are well below the reach of upcoming experiments.

5 Collider Signatures

In HENS scenarios, the sleptons and the electroweak gauginos are generally very light relative to the squarks and the gluino. If the lightest neutralino is the LSP, which we assume throughout this section, the distinguishing feature of these scenarios at colliders are multi-lepton events with missing E_T . In this section we discuss the prospects for discovery and identification of HENS models at the Tevatron and the LHC.

5.1 Trilepton Signature at the Tevatron

The most promising search channel at the Tevatron is the trilepton signal with missing E_T [64, 65, 66]. This can be induced, for example, by the electroweak production of $\chi_2^0 \chi_1^\pm$, with subsequent cascades of the form $\chi_2^0 \rightarrow \tilde{\ell}_L^* \ell^- \rightarrow \chi_1^0 \ell^+ \ell^+$ and $\chi_1^+ \rightarrow \tilde{\nu}_\ell \ell'^+ \rightarrow \chi_1^0 \nu_\ell \ell'^+$. For $M_{1/2} \geq 300$ GeV, the significant source of SUSY events comes from the electroweak production of gauginos, making this channel a copious and clean one. In HENS scenarios, the χ_2^0 and χ_1^\pm states tend to be mostly Wino and have two-body decays into left-handed sleptons. Because of this feature, the branching fractions of the abovementioned decay cascades can be significant, leading to a sizeable trilepton cross-section. Indeed, the mass spectrum derived from HENS models is close to being optimal for trilepton production.

To estimate the effective Tevatron trilepton cross-sections, we have simulated SUSY production from $p\bar{p}$ collisions at $\sqrt{s} = 1.96$ TeV using ISAJET 7.74 [67]. Following the treatment in Ref. [66], we use the ISAJET subroutines CALSIM and CALINI (in the ISAPLT package) as a simple detector model with coverage in the range $-4 < \eta < 4$, and calorimeter cells of size $\Delta\eta \times \Delta\phi = 0.1 \times 0.262$. To simulate energy resolution uncertainties, the electromagnetic calorimeter cells are smeared by an amount $0.15/\sqrt{E/\text{GeV}}$, while the hadronic calorimeter cells are smeared by an amount $0.7/\sqrt{E/\text{GeV}}$. We define jets as hadronic clusters with $E_T > 15$ GeV within a cone of size $\Delta R = 0.7$, and use the GETJET subroutine to perform the clustering. Isolated leptons are defined to be e 's or μ 's having $p_T > 5$ GeV, with net visible hadronic activity $E_T < 2$ GeV within a cone of size $\Delta R = 0.4$ about the lepton direction.

We focus on a particular set of cuts, corresponding to the HC2 set in Ref. [66], that is well-suited to the HENS mass spectrum [65, 68]. In each event, we require three isolated leptons with $p_T(\ell_{1,2,3}) > 20, 15, 10$ GeV, and $|\eta(\ell_{1,2,3})| < 2.5$. In addition to this, the total missing E_T must exceed 25 GeV, the invariant mass of same-flavor opposite-sign dileptons must lie in the range $12 \text{ GeV} < m_{\ell\ell} < 81 \text{ GeV}$, and the transverse invariant mass between each lepton and the missing E_T vector must lie outside the range $60 \text{ GeV} < m_T(\ell, \cancel{E}_T) < 85 \text{ GeV}$. The dilepton invariant mass veto is designed to remove background events from off-shell Z and γ decays, while the m_T veto removes leptons from W decays. With these cuts, the SM background is estimated to be 0.49 fb [66], and is due mostly to the remaining W^*Z^* and $W^*\gamma^*$ events in which both off-shell gauge bosons decay leptonically.

In Fig. 12 we show the trilepton cross-section subject to the cuts for $M_{1/2} = 300$ GeV and $\tan\beta = 10$. This value of $M_{1/2}$ is about as small as possible within the model given the lower bound on the light Higgs boson mass, and represents a best-case scenario at the Tevatron. Note that for considerably larger values of $\tan\beta$, the constraint from the anomalous magnetic moment of the muon requires larger values of $M_{1/2}$ as well, as can be seen in Fig. 5. Like in the previous plots, the values of $m_{H_u}^2$ and $m_{H_d}^2$ in Fig. 12 are those at the input scale, $M_c = M_{GUT}$.

The dependence of the trilepton cross-section on $m_{H_u}^2$ and $m_{H_d}^2$ can be understood in terms of the mass spectrum. Except in the upper-right portion of the allowed parameter space, the effective cross-section increases smoothly from bottom to top as the value of μ decreases. In most of the parameter space, μ is larger than M_2 and the χ_2^0 and χ_1^\pm states

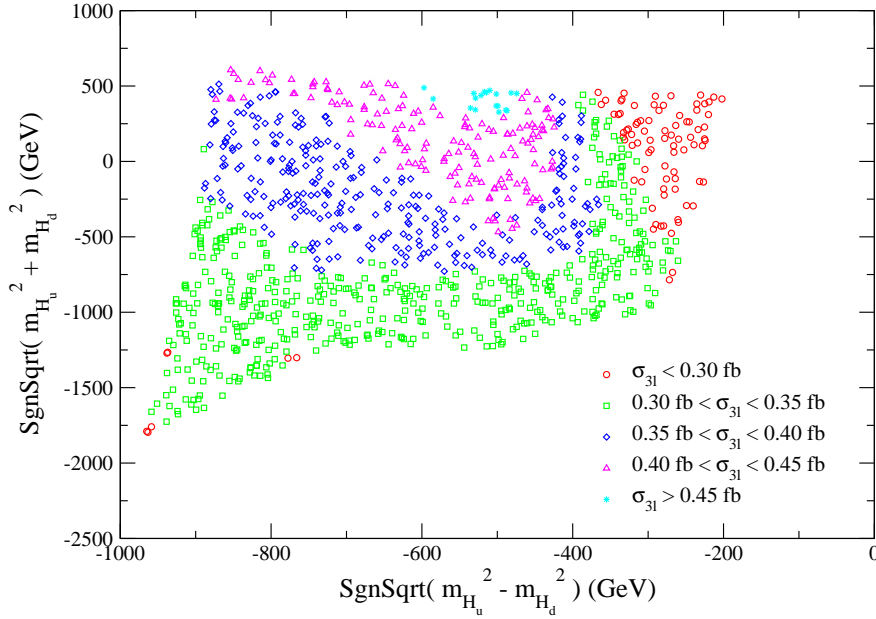


Figure 12: Trilepton cross-sections after HC2 cuts at the Tevatron for $M_{1/2} = 300$ GeV and $\tan\beta = 10$. The estimated background is $0.49 fb$ [66].

are mostly Wino. As μ approaches M_2 , these states develop a larger Higgsino fraction and their masses are reduced by the mixing. The heavier chargino and neutralino states become lighter as well. On account of these effects, the total gaugino cross section is increased leading to more trilepton events. This pattern is broken in the upper right corner of the parameter space because the mass of the χ_2^0 state approaches the left-handed slepton masses from above, again due to Higgsino mixing. When this mass difference becomes small, the branching fraction for $\chi_2^0 \rightarrow \ell_L \ell$ goes down. The leptons produced by the cascades become relatively soft as well. Since this decay mode plays a prominent role in the trilepton signal subject to the HC2 cuts, the effective cross-section falls off rapidly when the decay fraction is suppressed. The effective cross-section in this region can be increased by using slightly weaker lepton p_T cuts, such as the SC2 set discussed in Ref. [66], but at the expense of an increase in background.

The effective trilepton cross-sections shown in Fig. 12 fall within the range of $0.2\text{--}0.5 fb$. Given the estimated background of $0.49 fb$, the signal significance level is marginal. For example, the Poisson probability P_p for a total of ten events, corresponding to the maximal expected signal and background with $10 fb^{-1}$, is about $P_p = 0.016$. While this is unfortunately not enough for a discovery, an excess of clean trilepton events at the Tevatron would provide a tantalizing hint of a light HENS scenario. We also note that other event signatures involving leptons can be searched for in these scenarios. Of particular noteworthiness is the same-sign dilepton signature, which has small standard model background.

5.2 Signals at the LHC

If nature is supersymmetric and has a HENS spectrum, the prospects for discovery at the LHC with 10 fb^{-1} of data are excellent provided $M_{1/2}$ is less than about 700 GeV. To quantify this, we focus on six inclusive LHC SUSY search channels, classified by the number of isolated leptons in the event: $0\ell + \cancel{E}_T + jets$; $1\ell + \cancel{E}_T + jets$; $2\ell OS + \cancel{E}_T + jets$; $2\ell SS + \cancel{E}_T + jets$; $3\ell + \cancel{E}_T + jets$; $\geq 4\ell + \cancel{E}_T + jets$ [69, 70]. (Here, *OS* and *SS* refer to opposite-sign and same-sign dileptons, respectively.) Besides an excess of events in these channels, which is expected in many SUSY scenarios, the relative numbers of events within different channels can point towards small input scalar soft masses.

Supersymmetric events at the LHC were simulated using ISAJET 7.74 [67]. We use the ISAJET subroutines CALSIM and CALINI (in the ISAPLT package) as a simple detector model with coverage in the range $|\eta| < 5$, and calorimeter cells of size $\Delta\eta \times \Delta\phi = 0.05 \times 0.05$. A gaussian smearing of the calorimeter cells is included to simulate energy resolution uncertainties. The electromagnetic calorimeter cells are smeared by an amount $0.1/\sqrt{E/\text{GeV}} \oplus 0.01$, where \oplus denotes addition in quadrature. Hadronic calorimeter cells are smeared by an amount $0.5/\sqrt{E/\text{GeV}} \oplus 0.03$ for $|\eta| < 3$, and $1.0/\sqrt{E/\text{GeV}} \oplus 0.07$ for $|\eta| > 3$. We define jets as clusters with $E_T > 100$ GeV and $|\eta| < 3$ within a cone of size $\Delta R = 0.7$, and use the GETJET subroutine to perform the clustering. Isolated leptons are defined to be e 's or μ 's having $p_T > 10$ GeV and $|\eta| < 2.5$, with total visible activity $E_T < 5$ GeV within a cone of size $\Delta R = 0.3$ about the lepton direction.

For all channels studied, we choose a cut energy $E_T^c = 200$ GeV and demand that each event have at least two hard jets, $n_j \geq 2$, with $E_T > E_T^c$, as well as missing transverse energy $\cancel{E}_T > E_T^c$. This cut substantially reduces the SM backgrounds relative to the SUSY signals.⁹ We also require that the transverse sphericity of the event satisfies $S_T > 0.2$ to reduce the dijet background [71]. In zero-lepton events, we demand that the transverse angle between the missing momentum vector and the nearest jet must lie in the range $30^\circ < \Delta\phi(\cancel{E}_T, j) < 90^\circ$. In the one-lepton channel, we require a single isolated lepton with $p_T > 20$ GeV, as well as $M_T(\ell, \cancel{E}_T) > 100$ GeV to reduce the leptonic W background. For events with two or more isolated leptons, we demand that $p_T(\ell_{1,2}) > 20$ GeV for the two hardest leptons.

The cross sections after cuts for $M_{1/2} = 500$ GeV and $\tan\beta = 10$ are given in Fig. 13 for five sample points. For comparison, the SM backgrounds are estimated to be about 400 fb , 26 fb , 9 fb , 0.25 fb , 0.1 fb , and 0.002 fb for the 0ℓ , 1ℓ , $2\ell OS$, $2\ell SS$, 3ℓ , and 4ℓ channels respectively [69, 70]. The locations of the sample points, *A*, *B*, *C*, *D*, and *E*, in the $m_{H_u}^2(M_{GUT}) - m_{H_d}^2(M_{GUT})$ plane are listed in the Appendix, and are also indicated in Figs. 14 and 15. Among the five sample points, *A* and *C* have a neutralino relic density within the WMAP allowed range, while the other points lead to relic densities that are too large (but could be acceptable with a non-standard cosmology). At point *E*, the μ term is on the same order as $M_2 \simeq 2M_1$, but it is greater than 750 GeV at the other sample points.

⁹A larger value of E_T^c would be preferable to reduce the large SM backgrounds in the 0ℓ channel. However, the 0ℓ SUSY signal is still easily distinguishable from the large background for the parameter points we consider here.

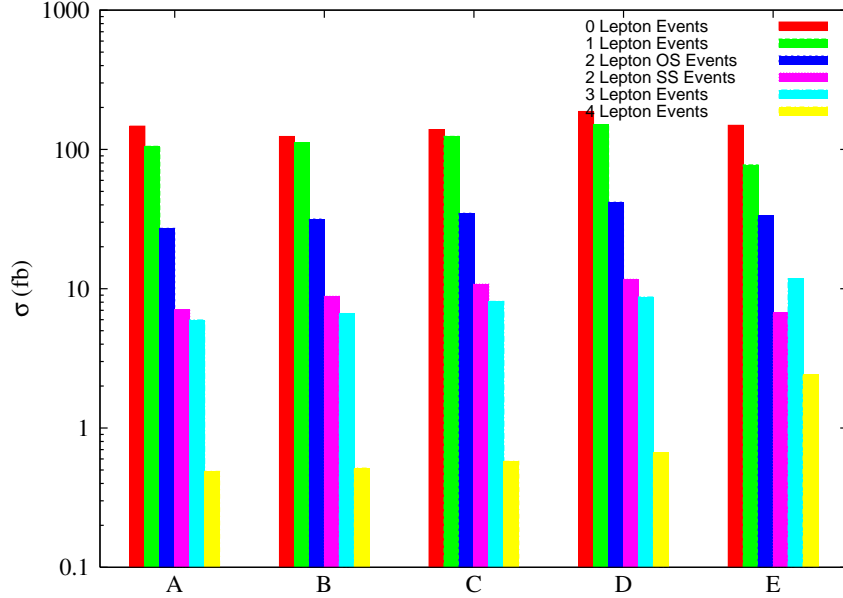


Figure 13: Inclusive signal cross-sections after cuts at the LHC for $M_{1/2} = 500$ GeV and $\tan\beta = 10$ for the five sample points described in the text. For comparison, the SM backgrounds are estimated to be about 400 fb, 26 fb, 9 fb, 0.25 fb, 0.1 fb, and 0.002 fb for the 0ℓ , 1ℓ , 2ℓ OS, 2ℓ SS, 3ℓ and 4ℓ channels respectively [69, 70].

Thus, except for point E, the LSP is a mostly Bino neutralino, while the lightest chargino and the next-to-lightest neutralino are predominantly Wino. At point E where $\mu < M_2$, all the chargino and neutralino states are fairly light and have significant Higgsino components, which, as we shall discuss below, is the reason for the increase in the 3ℓ and 4ℓ rates.

In each of the six search channels, the SUSY signal is easily distinguishable from the background with $10fb^{-1}$ of luminosity at the LHC. A more challenging task beyond an initial discovery is to distinguish this class of models from other (SUSY) scenarios and to deduce the model parameters. The number of leptonic events relative to the number of 0ℓ events is useful in this regard. Compared to a generic mSUGRA input spectrum with $m_0 > 0$, the ratio of 1ℓ events to 0ℓ events is much larger for a given value of $M_{1/2}$. For example, in mSUGRA with $(m_0, M_{1/2}, A_0, \tan\beta, sgn(\mu)) = (200 \text{ GeV}, 500 \text{ GeV}, 0, 10, +)$, the ratio of 0ℓ to 1ℓ events is greater than four, whereas this ratio is close to unity for all five sample points considered. The ratio of the number of 0ℓ events to the number of 2ℓ events is also much larger in a generic mSUGRA framework than it is here. This is the consequence of having left-handed sleptons lighter than the χ_2^0 and χ_1^\pm states, which are in turn light enough to be generated by squark decays. For example, cascade chains such as $\tilde{q} \rightarrow \chi_2^0 q \rightarrow \tilde{\ell}_L^* \ell^- q \rightarrow \chi_1^0 \ell^+ \ell^- q$ have a significant branching probability, and are a rich source of leptons.

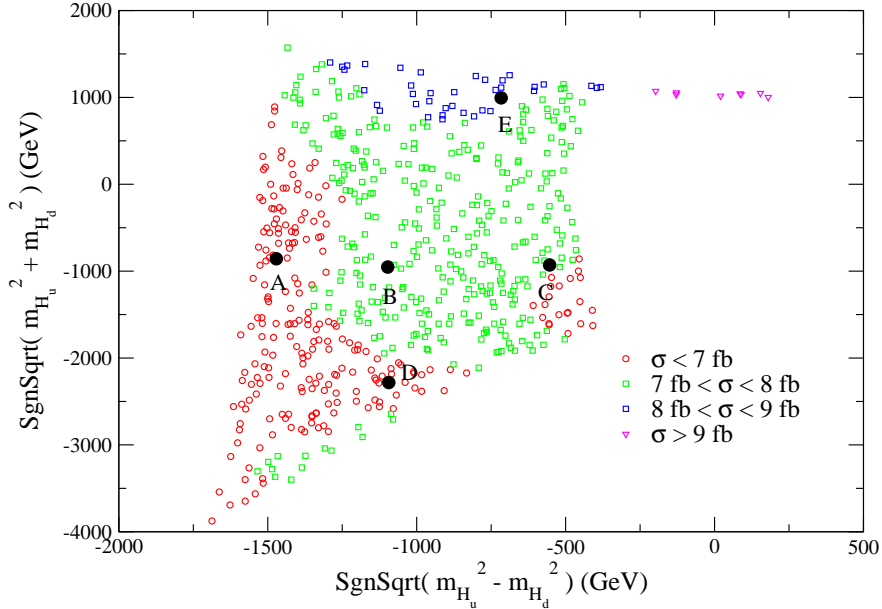


Figure 14: 3ℓ cross-sections after cuts at the LHC for $M_{1/2} = 500$ GeV and $\tan\beta = 10$. The estimated background is $0.1 fb$.

The dependence of the effective 3ℓ cross-section on the input Higgs soft mass parameters is shown in Fig. 14. For the most part, this dependence is fairly mild except in the upper right portion of the allowed region. Here, the μ term approaches the Bino mass M_1 , and in the thin tail extending to the right, μ even falls below M_1 . In this region, all the neutralinos and charginos are significantly lighter than the squarks and gluinos. As a result, the decay cascades initiated by the strong superpartners are frequently very long, involving several chargino and neutralino states. At each step in the cascade chain there is a chance of producing a lepton, and thus the total fraction of events containing multiple leptons is very high. For example, the decay chain $\tilde{u}_R \rightarrow \chi_3^0 u \rightarrow \tilde{\ell}_R^* \ell^- u \rightarrow \chi_1^0 \ell^+ \ell^- u$ is kinematically allowed when μ is small, and has a significant branching fraction. The preponderance of leptons can be so high that the number of 0ℓ and 1ℓ events (and even to some extent some 2ℓ events) are significantly suppressed. This can be seen in Fig. 15, which shows the 1ℓ effective cross section for $M_{1/2} = 500$ GeV and $\tan\beta = 10$. Note that the small μ region is strongly constrained by direct and indirect searches for dark matter, and will be probed by upcoming experiments, as was discussed above.

In the leftmost portion of the allowed region of Fig. 14, there is also a net decrease in the cross section, which occurs in the other leptonic channels as well. Within this region, leptons typically originate from decays of the mostly Wino χ_2^0 and χ_1^\pm states into left-handed sleptons and sneutrinos, which subsequently decay into the neutralino LSP. However, these left-handed states are only slightly heavier than the LSP, so the lepton emitted from the

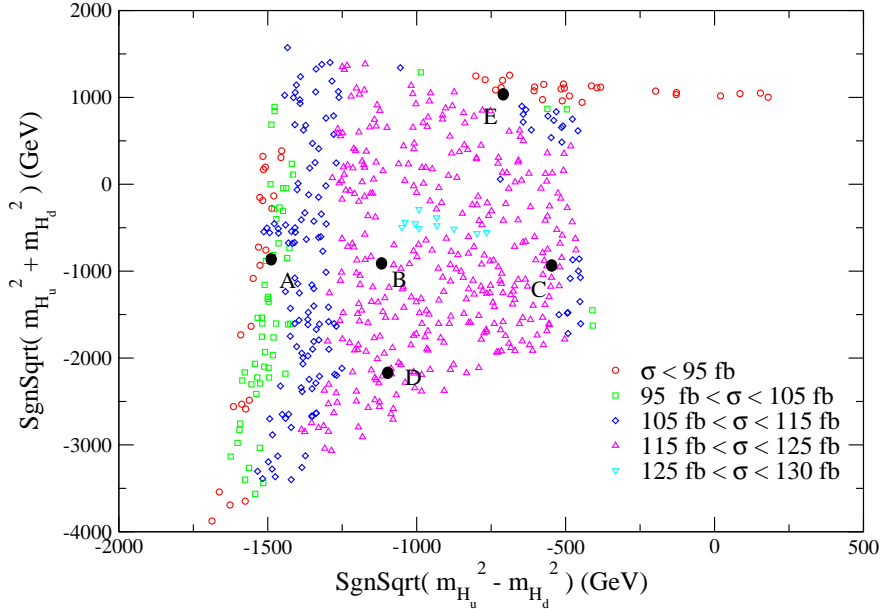


Figure 15: 1ℓ cross-sections after cuts at the LHC for $M_{1/2} = 500$ GeV and $\tan\beta = 10$. The estimated background is $26 fb$.

slepton decays tends to be soft, making it less likely to pass the lepton p_T cuts.

A particularly distinctive signature of the HENS models are inclusive 4ℓ events. We find effective cross-sections above $0.5 fb$ for $\tan\beta = 10$ and $M_{1/2} = 500$ GeV, which is sufficient for a $10 fb^{-1}$ LHC discovery given the SM background of about $0.002 fb$ [70]. There is a sharp increase in the 4ℓ cross-section in the small μ region at the upper right of the parameter space. The dominant sources of this increase are cascades initiated by right-handed squarks of the type described previously. Furthermore, because the left-handed sleptons are lighter than χ_3^0 but heavier than χ_2^\pm and χ_4^0 in this region, superpartner cascades such as $\tilde{u}_L \rightarrow \chi_2^\pm \rightarrow \tilde{\nu} \rightarrow \chi_3^0 \rightarrow \tilde{\ell}_R \rightarrow \chi_1^0$ accompanied by many leptons have a non-trivial branching fraction and can produce three leptons from the single squark parent.¹⁰ As a result, 4ℓ rates greater than $5 fb$ can occur. We have also investigated the exclusive clean trilepton channel. It does not appear to be as promising as the inclusive channels.

Varying $\tan\beta$ does not qualitatively affect our findings. The cross sections after cuts for $M_{1/2} = 500$ GeV and $\tan\beta = 30$ are given in Fig. 16 for five sample points, A' , B' , C' , D' , E' . Details of these sample points are given in the Appendix. The cross sections in all six channels are similar to those in Fig. 13 with $\tan\beta = 10$. In particular, the ratio of 0ℓ to 1ℓ events is still close to unity, and the 3ℓ and 4ℓ rates are observably large. The main difference that

¹⁰The final lepton in this cascade tends to be quite soft because the mass difference ($m_{\tilde{\ell}_R} - m_{\chi_1^0}$) is very small in this part of the parameter space. However, the other two leptons in the cascade tend to be quite hard.

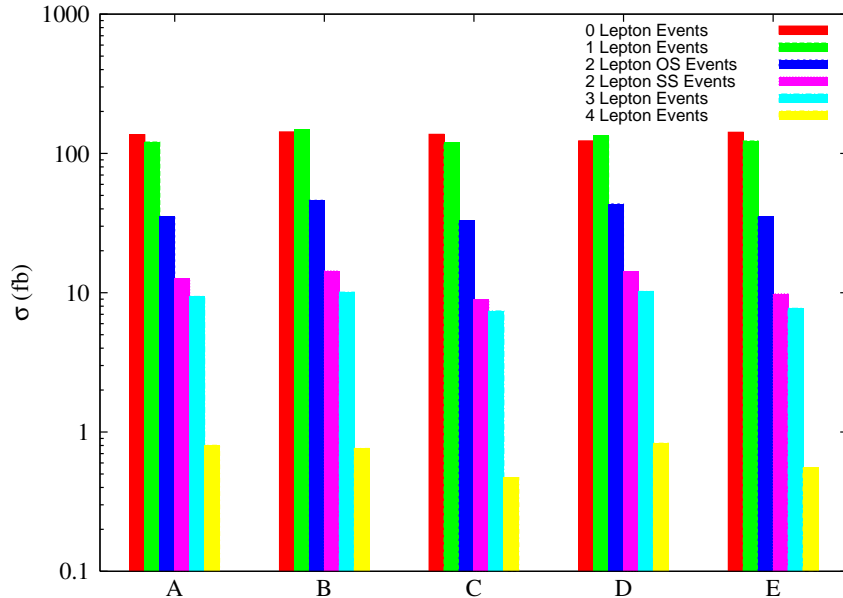


Figure 16: Inclusive signal cross-sections after cuts at the LHC for $M_{1/2} = 500$ GeV and $\tan\beta = 30$ for the five sample points described in the text. For comparison, the SM backgrounds are estimated to be about $400 fb$, $26 fb$, $9 fb$, $0.25 fb$, $0.1 fb$, and $0.002 fb$ for the 0ℓ , 1ℓ , $2\ell OS$, $2\ell SS$, 3ℓ and 4ℓ channels respectively [69, 70].

occurs at larger values of $\tan\beta$ is that there is no small μ region.

Since the entire mass spectrum in HENS models scales with $M_{1/2}$, so too do the event rates. We have checked that for $M_{1/2}$ as large 700 GeV, corresponding to a gluino mass of $m_{\tilde{g}} \simeq 1600$ GeV, the inclusive event rates in all channels other than the 0ℓ and 4ℓ are large enough that a discovery with $10fb^{-1}$ of LHC data is feasible. On the other hand, the event rates become even larger for smaller values of $M_{1/2}$, making discovery even easier.

6 Discussion

Supersymmetry has been recognized as a viable theory of physics beyond the Standard Model for many years now. It was quickly realized that it was not only viable, but also potentially useful in the quest to understand stability of the electroweak potential, radiative electroweak symmetry breaking, grand unification, dark matter, and baryogenesis. In subsequent years, there has been much effort devoted to understanding how supersymmetry breaking is to be achieved without creating additional phenomenological problems, such as too large FCNC.

There are two particularly simple alternatives that keep the good features of super-

symmetry while (mostly) dismissing the bad features. One approach is to raise the scalar masses significantly higher than the supersymmetric fermion masses. This is the idea of Split Supersymmetry discussed in the introduction. One drawback of this scenario is the apparent finetuning in the electroweak sector.

The approach we pursue in this article is in some sense the opposite of Split Supersymmetry. Here, rather than introduce a huge hierarchy of scalar masses over fermion masses, we wish to zero out the superpartner scalar masses at some scale (i.e., “Splat Supersymmetry”). The simplest model of all scalar masses having a zero boundary condition does not work. However, applying a small alteration to the most minimal idea, namely that the Higgs bosons are exempt from zero boundary condition requirement, preserves the good features of these theories, while satisfying the phenomenological requirements described in the text.

This idea of Higgs Exempt No-Scale (HENS) supersymmetry has many phenomenological implications worthy of consideration at current and future experimental facilities. For example, we have found that the scenario can accommodate the tantalizing (but small) deviation of $(g-2)$ of the muon compared to the SM prediction. It also suggests a near maximal leptonic signal for the Tevatron, and thus provides an excellent benchmark theory for the Tevatron to either discover this form of supersymmetry or rule out large regions of parameter space in a clean way. Furthermore, the LHC signatures are of many multi-lepton events. Perhaps the most distinctive of them is the inclusive 4ℓ channel which can effectively rule out HENS models up to gaugino mass scales that are uncomfortably large from the normal finetuning point of view. For the most part, this form of supersymmetry is rather straightforward for the LHC to find. An important exception is the lightest Higgs boson, whose mass is pressured in this scenario to be low, and thus perhaps close to the current bound of 114 GeV. Given the difficulties of finding a Higgs boson less than 120 GeV [72], discovering the Higgs boson might be one of the more challenging steps in confirming the complete structure of this theory.

Acknowledgements

We would like to thank P. Kumar for discussions, and for contributions at the early stages of this work. We also wish to thank G. Kane, S. Martin, A. Pierce and S. Thomas for helpful discussions. This work is supported in part by the Department of Energy and the Michigan Center for Theoretical Physics.

Appendix: Sample Point Parameters

In this appendix, we list the relevant properties of the sample points A, B, C, D, E chosen for $\tan\beta = 10$ and $M_{1/2} = 500$ GeV. The locations of these points in the $Sgn.Sqrt(m_{H_u}^2 \pm m_{H_d}^2)$ plane are shown in Figs. 14 and 15. We also list properties of the points A', B', C', D', E' corresponding to $\tan\beta = 30$ and $M_{1/2} = 500$ GeV.

	<i>A</i>	<i>B</i>	<i>C</i>	<i>D</i>	<i>E</i>
<i>Sgn.Sqrt</i> (-)	-1480	-1103	-530	-1087	-712
<i>Sgn.Sqrt</i> (+)	-820	-921	-900	-2138	1197
μ	1150	1033	868	1523	278
M_{A^0}	1465	1156	764	854	1060
M_1	210	210	210	210	209
M_2	389	389	389	389	398
$m_{\chi_1^0}$	209	209	209	210	193
$m_{\chi_2^0}$	385	385	383	387	266
$m_{\chi_3^0}$	1152	1034	871	1525	283
$m_{\chi_4^0}$	1156	1040	878	1527	420
$m_{\chi_1^\pm}$	385	385	383	387	254
$m_{\chi_2^\pm}$	1157	1041	878	1528	419
$m_{\tilde{\nu}_e}$	223	274	315	281	304
$m_{\tilde{e}_L}$	237	285	325	292	314
$m_{\tilde{e}_R}$	384	312	223	308	249
$m_{\tilde{\nu}_\tau}$	217	272	315	288	298
$m_{\tilde{\tau}_1}$	221	261	214	261	233
$m_{\tilde{\tau}_2}$	383	328	331	352	310
$m_{\tilde{g}}$	1156	1155	1152	1161	1151
$m_{\tilde{t}_1}$	901	875	837	1027	719
$m_{\tilde{t}_2}$	1069	1046	1017	1163	955
$m_{\tilde{u}_L}$	1019	1016	1012	1007	1020
$m_{\tilde{u}_R}$	933	952	969	943	972
Ωh^2	0.098	0.687	0.096	0.642	0.134

Table 1: Model parameters and particle masses for sample points *A, B, C, D, E*, all with $\tan\beta = 10$ and $M_{1/2} = 500$ GeV. All dimensionful quantities in the table are listed in GeV units. The Ωh^2 values are valid computations for the assumption of standard thermal cosmological evolution and stable lightest neutralino. Viability of points *B* and *D* require alterations to the standard assumptions.

	A'	B'	C'	D'	E'
$SgnSqrt(-)$	-1595	-1019	-501	-1334	-1270
$SgnSqrt(+)$	-3241	-2219	-1601	-2981	-2084
μ	2195	1547	1153	2003	1542
M_{A^0}	1031	768	522	826	1045
M_1	212	211	211	212	211
M_2	391	390	390	391	390
$m_{\chi_1^0}$	212	211	210	212	211
$m_{\chi_2^0}$	390	388	387	390	388
$m_{\chi_3^0}$	2197	1549	1156	2005	1544
$m_{\chi_4^0}$	2197	1550	1159	2006	1546
$m_{\chi_1^\pm}$	390	388	387	390	388
$m_{\chi_2^\pm}$	2197	1551	1159	2006	1547
$m_{\tilde{\nu}_e}$	220	287	318	256	260
$m_{\tilde{e}_L}$	234	298	327	270	272
$m_{\tilde{e}_R}$	403	296	219	353	342
$m_{\tilde{\nu}_\tau}$	384	360	357	394	315
$m_{\tilde{\tau}_1}$	320	272	233	324	232
$m_{\tilde{\tau}_2}$	643	494	425	599	482
$m_{\tilde{g}}$	1168	1162	1154	1168	1161
$m_{\tilde{t}_1}$	1235	1043	924	1179	1038
$m_{\tilde{t}_2}$	1393	1165	1063	1321	1160
$m_{\tilde{u}_L}$	1004	1008	1008	1005	1009
$m_{\tilde{u}_R}$	908	946	964	926	935
Ωh^2	0.105	0.521	0.0954	0.749	0.104

Table 2: Model parameters and particle masses for sample points A', B', C', D', E' , all with $\tan\beta = 30$ and $M_{1/2} = 500$ GeV. All dimensionful quantities in the table are listed in GeV units. The Ωh^2 values are valid computations for the assumption of standard thermal cosmological evolution and stable lightest neutralino. Viability of points B' and D' require alterations to the standard assumptions.

References

- [1] For reviews, see for example H. E. Haber and G. L. Kane, Phys. Rept. **117**, 75 (1985); S. P. Martin, hep-ph/9709356; D. J. H. Chung et al., Phys. Rept. **407**, 1 (2005) [hep-ph/0312378]; M. A. Luty, hep-th/0509029.
- [2] S. Dimopoulos and H. Georgi, Nucl. Phys. B **193**, 150 (1981).
- [3] S. Dimopoulos, S. Raby and F. Wilczek, Phys. Rev. D **24**, 1681 (1981).
- [4] See for example, F. Gabbiani, E. Gabrielli, A. Masiero and L. Silvestrini, Nucl. Phys. B **477**, 321 (1996) [hep-ph/9604387], M. Misiak, S. Pokorski and J. Rosiek, Adv. Ser. Direct. High Energy Phys. **15**, 795 (1998) [hep-ph/9703442].
- [5] M. Dugan, B. Grinstein and L. J. Hall, Nucl. Phys. B **255**, 413 (1985).
- [6] M. Brhlik, G. J. Good and G. L. Kane, Phys. Rev. D **59**, 115004 (1999) [hep-ph/9810457]; T. Ibrahim and P. Nath, Phys. Rev. D **61**, 093004 (2000) [hep-ph/9910553].
- [7] M. Leurer, Y. Nir and N. Seiberg, Nucl. Phys. B **398**, 319 (1993) [hep-ph/9212278]. Y. Nir and N. Seiberg, Phys. Lett. B **309**, 337 (1993) [hep-ph/9304307]. M. Leurer, Y. Nir and N. Seiberg, Nucl. Phys. B **420**, 468 (1994) [hep-ph/9310320]. M. Dine, R. G. Leigh and A. Kagan, Phys. Rev. D **48**, 4269 (1993) [hep-ph/9304299]. L. J. Hall and H. Murayama, Phys. Rev. Lett. **75**, 3985 (1995) [hep-ph/9508296]. R. Barbieri, G. R. Dvali and L. J. Hall, Phys. Lett. B **377**, 76 (1996) [hep-ph/9512388]. R. Barbieri, L. J. Hall and A. Romanino, Phys. Lett. B **401**, 47 (1997) [hep-ph/9702315].
- [8] For a review, see G. F. Giudice and R. Rattazzi, Phys. Rept. **322**, 419 (1999) [hep-ph/9801271], and references therein.
- [9] L. Randall and R. Sundrum, Nucl. Phys. B **557**, 79 (1999) [hep-th/9810155]. G. F. Giudice, M. A. Luty, H. Murayama and R. Rattazzi, JHEP **9812**, 027 (1998) [hep-ph/9810442].
- [10] J. D. Wells, [hep-ph/0306127]; Phys. Rev. D **71**, 015013 (2005) [hep-ph/0411041],
- [11] N. Arkani-Hamed and S. Dimopoulos, JHEP **0506**, 073 (2005) [hep-th/0405159]. G. F. Giudice and A. Romanino, Nucl. Phys. B **699**, 65 (2004) [Erratum-ibid. B **706**, 65 (2005)] [hep-ph/0406088]. N. Arkani-Hamed, S. Dimopoulos, G. F. Giudice and A. Romanino, Nucl. Phys. B **709**, 3 (2005) [hep-ph/0409232].
- [12] See also A. Pierce, Phys. Rev. D **70**, 075006 (2004) [hep-ph/0406144]. A. Arvanitaki and P. W. Graham, Phys. Rev. D **72**, 055010 (2005) [hep-ph/0411376]. A. Masiero, S. Profumo and P. Ullio, Nucl. Phys. B **712**, 86 (2005) [hep-ph/0412058]. B. Thomas, Phys. Rev. D **72**, 023519 (2005) [hep-ph/0503248]. N. Arkani-Hamed, A. Delgado and G. F. Giudice, Nucl. Phys. B **741**, 108 (2006) [hep-ph/0601041]. U. Chattopadhyay, D. Das, P. Konar and D. P. Roy, hep-ph/0610077. M. Ibe, T. Moroi and T. T. Yanagida, hep-ph/0610277. R. Mahbubani and L. Senatore, Phys. Rev. D **73**, 043510 (2006) [hep-ph/0510064].

- [13] M. Dine, A. Kagan and S. Samuel, Phys. Lett. B **243**, 250 (1990).
- [14] D. E. Kaplan, G. D. Kribs and M. Schmaltz, Phys. Rev. D **62**, 035010 (2000) [hep-ph/9911293]; Z. Chacko, M. A. Luty, A. E. Nelson and E. Ponton, JHEP **0001**, 003 (2000) [hep-ph/9911323].
- [15] For a review, see A. B. Lahanas and D. V. Nanopoulos, Phys. Rept. **145**, 1 (1987); A. B. Lahanas, CERN-TH-7092-93 *Lectures given at International School of Subnuclear Physics: 31th Course: From Supersymmetry to the Origin of Space-Time, Erice, Italy, 4- 12 Jul 1993*
- [16] M. A. Luty and R. Sundrum, Phys. Rev. D **65**, 066004 (2002) [hep-th/0105137]. M. Luty and R. Sundrum, Phys. Rev. D **67**, 045007 (2003) [hep-th/0111231]. M. Ibe, K. I. Izawa, Y. Nakayama, Y. Shinbara and T. Yanagida, Phys. Rev. D **73**, 015004 (2006) [hep-ph/0506023]. M. Ibe, K. I. Izawa, Y. Nakayama, Y. Shinbara and T. Yanagida, Phys. Rev. D **73**, 035012 (2006) [hep-ph/0509229]. M. Schmaltz and R. Sundrum, hep-th/0608051.
- [17] M. Schmaltz and W. Skiba, Phys. Rev. D **62**, 095005 (2000) [hep-ph/0001172].
- [18] M. Schmaltz and W. Skiba, Phys. Rev. D **62**, 095004 (2000) [hep-ph/0004210].
- [19] D. E. Kaplan and T. M. P. Tait, JHEP **0006**, 020 (2000) [hep-ph/0004200].
- [20] W. Buchmuller, J. Kersten and K. Schmidt-Hoberg, JHEP **0602**, 069 (2006) [hep-ph/0512152].
- [21] S. Komine and M. Yamaguchi, Phys. Rev. D **63**, 035005 (2001) [hep-ph/0007327]. C. Balazs and R. Dermisek, JHEP **0306**, 024 (2003) [hep-ph/0303161].
- [22] W. Buchmuller, L. Covi, J. Kersten and K. Schmidt-Hoberg, [hep-ph/0609142].
- [23] For a recent discussion of negative values of m_0 in mSUGRA, see: J. L. Feng, A. Rajaraman and B. T. Smith, Phys. Rev. D **74**, 015013 (2006) [hep-ph/0512172].
- [24] E. Cremmer, S. Ferrara, C. Kounnas and D. V. Nanopoulos, Phys. Lett. B **133**, 61 (1983).
- [25] J. R. Ellis, A. B. Lahanas, D. V. Nanopoulos and K. Tamvakis, Phys. Lett. B **134**, 429 (1984).
- [26] J. R. Ellis, C. Kounnas and D. V. Nanopoulos, Nucl. Phys. B **241**, 406 (1984).
- [27] J. R. Ellis, C. Kounnas and D. V. Nanopoulos, Nucl. Phys. B **247**, 373 (1984).
- [28] See, for example, N. Weiner, hep-ph/0106097; C. Csaki, G. D. Kribs and J. Terning, Phys. Rev. D **65**, 015004 (2002) [hep-ph/0107266].
- [29] E. Witten, Phys. Lett. B **155**, 151 (1985). P. G. Camara, L. E. Ibanez and A. M. Uranga, Nucl. Phys. B **689**, 195 (2004) [hep-th/0311241]. K. Choi, A. Falkowski, H. P. Nilles and M. Olechowski, Nucl. Phys. B **718**, 113 (2005) [hep-th/0503216].

- [30] M. Dine, P. J. Fox, E. Gorbatov, Y. Shadmi, Y. Shirman and S. D. Thomas, Phys. Rev. D **70**, 045023 (2004) [hep-ph/0405159].
- [31] A. E. Nelson and M. J. Strassler, JHEP **0009**, 030 (2000) [hep-ph/0006251].
- [32] A. E. Nelson and M. J. Strassler, JHEP **0207**, 021 (2002) [hep-ph/0104051].
- [33] T. Kobayashi and H. Terao, Phys. Rev. D **64**, 075003 (2001) [hep-ph/0103028].
- [34] T. Kobayashi, H. Nakano, T. Noguchi and H. Terao, Phys. Rev. D **66**, 095011 (2002) [hep-ph/0202023].
- [35] K. R. Dienes, E. Dudas and T. Gherghetta, Phys. Lett. B **436**, 55 (1998) [hep-ph/9803466]; K. R. Dienes, E. Dudas and T. Gherghetta, Nucl. Phys. B **537**, 47 (1999) [hep-ph/9806292].
- [36] A. E. Nelson and M. J. Strassler, Phys. Rev. D **56**, 4226 (1997) [hep-ph/9607362].
- [37] S. P. Martin and M. T. Vaughn, Phys. Rev. D **50**, 2282 (1994) [hep-ph/9311340].
- [38] A. Djouadi, J. L. Kneur and G. Moultaka, [hep-ph/0211331].
- [39] W. M. Yao *et al.* [Particle Data Group], J. Phys. G **33**, 1 (2006).
- [40] E. Brubaker *et al.* [Tevatron Electroweak Working Group], hep-ex/0608032.
- [41] E. Barberio *et al.* [Heavy Flavor Averaging Group (HFAG)], hep-ex/0603003.
- [42] See, for example, J. A. Casas, A. Lleyda and C. Munoz, Nucl. Phys. B **471**, 3 (1996) [hep-ph/9507294].
- [43] A. Kusenko, P. Langacker and G. Segre, Phys. Rev. D **54**, 5824 (1996) [hep-ph/9602414]. M. Carena, M. Quiros and C. E. M. Wagner, Phys. Lett. B **380**, 81 (1996) [hep-ph/9603420]. T. Falk, K. A. Olive, L. Roszkowski, A. Singh and M. Srednicki, Phys. Lett. B **396**, 50 (1997) [hep-ph/9611325].
- [44] S. Komine, T. Moroi and M. Yamaguchi, Phys. Lett. B **507**, 224 (2001) [hep-ph/0103182].
- [45] T. Moroi, Phys. Rev. D **53**, 6565 (1996) [Erratum-ibid. D **56**, 4424 (1997)] [hep-ph/9512396].
- [46] R. Barate *et al.* [LEP Working Group for Higgs boson searches], Phys. Lett. B **565**, 61 (2003) [hep-ex/0306033].
- [47] D. E. Morrissey and J. D. Wells, Phys. Rev. D **74**, 015008 (2006) [hep-ph/0512019].
- [48] See R. Barbieri and G. F. Giudice, Nucl. Phys. B **306**, 63 (1988), and references thereto.
- [49] A. Gould, B. T. Draine, R. W. Romani and S. Nussinov, Phys. Lett. B **238**, 337 (1990); A. De Rujula, S. L. Glashow and U. Sarid, Nucl. Phys. B **333**, 173 (1990); S. Dimopoulos, D. Eichler, R. Esmailzadeh and G. D. Starkman, Phys. Rev. D **41**, 2388 (1990).

- [50] T. Falk, K. A. Olive and M. Srednicki, Phys. Lett. B **339**, 248 (1994) [hep-ph/9409270].
- [51] L. J. Hall, T. Moroi and H. Murayama, Phys. Lett. B **424**, 305 (1998) [hep-ph/9712515]. N. Arkani-Hamed, L. J. Hall, H. Murayama, D. R. Smith and N. Weiner, Phys. Rev. D **64**, 115011 (2001) [hep-ph/0006312]. D. Hooper, J. March-Russell and S. M. West, Phys. Lett. B **605**, 228 (2005) [hep-ph/0410114]. T. Asaka, K. Ishiwata and T. Moroi, Phys. Rev. D **73**, 051301 (2006) [hep-ph/0512118]. S. Gopalakrishna, A. de Gouvea and W. Porod, JCAP **0605**, 005 (2006) [hep-ph/0602027].
- [52] For a nice review of these scenarios, see: J. L. Feng, Annals Phys. **315** (2005) 2.
- [53] P. Gondolo, J. Edsjo, P. Ullio, L. Bergstrom, M. Schelke and E. A. Baltz, JCAP **0407**, 008 (2004) [astro-ph/0406204].
- [54] D. N. Spergel *et al.*, [astro-ph/0603449].
- [55] For some recent examples, see G. Gelmini, P. Gondolo, A. Soldatenko and C. E. Yaguna, Phys. Rev. D **74**, 083514 (2006) [hep-ph/0605016]. D. E. Morrissey and J. D. Wells, hep-ph/0606234.
- [56] D. S. Akerib *et al.*, Nucl. Instrum. Meth. A **559**, 390 (2006).
- [57] J. R. Ellis, A. D. Linde and D. V. Nanopoulos, Phys. Lett. B **118**, 59 (1982).
- [58] See, for example, M. Dine, R. Kitano, A. Morisse and Y. Shirman, Phys. Rev. D **73**, 123518 (2006) [hep-ph/0604140], and references therein.
- [59] J. L. Feng, S. f. Su and F. Takayama, Phys. Rev. D **70**, 063514 (2004) [hep-ph/0404198]; J. L. Feng, S. Su and F. Takayama, Phys. Rev. D **70**, 075019 (2004) [hep-ph/0404231].
- [60] See, for example, H. Baer, A. Belyaev, T. Krupovnickas and J. O’Farrill, JCAP **0408**, 005 (2004) [hep-ph/0405210]; J. R. Ellis, K. A. Olive, Y. Santoso and V. C. Spanos, Phys. Rev. D **71**, 095007 (2005) [hep-ph/0502001].
- [61] S. Desai *et al.* [Super-Kamiokande Collaboration], Phys. Rev. D **70**, 083523 (2004) [Erratum-ibid. D **70**, 109901 (2004)] [hep-ex/0404025].
- [62] P. A. Toale [IceCube Collaboration], [astro-ph/0607003].
- [63] J. Hossl [ANTARES Collaboration], *Prepared for IDM 2004: 5th International Workshop on the Identification of Dark Matter, Edinburgh, Scotland, United Kingdom, 6-10 Sep 2004*
- [64] See, for example, H. Baer and X. Tata, Phys. Rev. D **47**, 2739 (1993); S. Mrenna, G. L. Kane, G. D. Kribs and J. D. Wells, Phys. Rev. D **53**, 1168 (1996) [hep-ph/9505245]; V. D. Barger, C. Kao and T. j. Li, Phys. Lett. B **433**, 328 (1998) [hep-ph/9804451]; E. Accomando, R. Arnowitt and B. Dutta, Phys. Lett. B **475**, 176 (2000) [hep-ph/9811300]; V. D. Barger and C. Kao, Phys. Rev. D **60**, 115015 (1999) [hep-ph/9811489]; J. D. Lykken and K. T. Matchev, Phys. Rev. D **61**, 015001 (2000) [hep-ph/9903238].

- [65] K. T. Matchev and D. M. Pierce, Phys. Rev. D **60**, 075004 (1999) [hep-ph/9904282];
K. T. Matchev and D. M. Pierce, Phys. Lett. B **467**, 225 (1999) [hep-ph/9907505].
- [66] H. Baer, M. Drees, F. Paige, P. Quintana and X. Tata, Phys. Rev. D **61**, 095007 (2000)
[hep-ph/9906233].
- [67] F. E. Paige, S. D. Protopopescu, H. Baer and X. Tata, hep-ph/0312045.
- [68] H. Baer, A. Belyaev, T. Krupovnickas and X. Tata, Phys. Rev. D **65**, 075024 (2002)
[hep-ph/0110270].
- [69] H. Baer, C. h. Chen, F. Paige and X. Tata, Phys. Rev. D **52**, 2746 (1995)
[hep-ph/9503271].
- [70] H. Baer, C. h. Chen, F. Paige and X. Tata, Phys. Rev. D **53**, 6241 (1996)
[hep-ph/9512383].
- [71] ATLAS detector and physics performance. Technical design report. Vol. 2, CERN-
LHCC-99-15, ATLAS-TDR-15, May 1999.
- [72] S. Asai *et al.* (ATLAS Collaboration), Eur. Phys. J. C **32S2**, 19 (2004)
[hep-ph/0402254]. S. Abdullin *et al.* (CMS Collaboration), Eur. Phys. J. C **39S2**, 41
(2005).